BSC

Design Calculation or Analysis Cover Sheet

Complete only applicable items.

1. QA: QA
2. Page 1 of 42

3. System	4. Document Identifier
Monitored Geologic Repository	000-00C-MGR0-04400-000-00A

5. Title

Drift Collapse Weight and Thermal Loading of TAD and 5-DHLW/DOE SNF Short Co-Disposal Waste Packages

6. Group

Thermal Structural Analysis Discipline

7. Document Status Designation

☐ Preliminary ☒ Committed ☐ Confirmed ☐ Cancelled/Superseded

8. Notes/Comments

Sections 1, 2, 3, 4, 5, 6.1, 6.2 , and Attachment I of the report have been prepared by Nakachew Alemu
Sections 6.3, 7, and Attachment II (CD) of this document have been prepared by Sripathi Nilkar

Attachments	Total Number of Pages
See Section 5	N/A

RECORD OF REVISIONS

9. No.	10. Reason For Revision	11. Total # of Pgs.	12. Last Pg. #	13. Originator (Print/Sign/Date)	14. Checker (Print/Sign/Date)	15. EGS (Print/Sign/Date)	16. Approved/Accepted (Print/Sign/Date)
00A	Initial Issue	42	I-3	Sripathi Nilkar 10/30/2007 Nakachew Alemu 10/30/2007	Mohan Durani 10/30/2007	Jason Viggato 10/30/2007	10/30/07

DISCLAIMER

The calculations contained in this document were developed by Bechtel SAIC Company, LLC (BSC) and are intended solely for the use of BSC in its work for the Yucca Mountain Project.

CONTENTS

Page

FIGURES

Page

TABLES

Page

ACRONYMS

ASME	American Society of Mechanical Engineers
ASTM	American Society for Testing and Materials
ASM	American Society of Metals
BSC	Bechtel SAIC Company, LLC
CPU	Central Processing Unit
CRWMS	Civilian Radioactive Waste Management System
CRWMS M&O	CRWMS Management and Operating Contractor
DHLW	Defense High Level Radioactive Waste
DOE	U.S. Department of Energy
EP	Emplacement Pallet
EWA	Elemental Wall Average
FEA	Finite Element Analysis
FE	Finite Element
FEM	Finite Element Model
FER	Finite Element Representation
HP	Hewlett-Packard
IV	Inner Vessel
LA	License Application
OCB	Outer Corrosion Barrier
RT	Room Temperature
SI	Stress Intensity
SNF	Spent Nuclear Fuel
SS	Stainless Steel
STN	Software Tracking Number
RED	Repository Emplacement Drift
TAD	Transportation, Aging, and Disposal
UNS	Unified Numbering System
WP	Waste Package

1. PURPOSE

The purpose of this calculation is to determine the structural response of the Transportation, Aging, Disposal (TAD) waste package (WP) and the 5–Defense High-Level Radioactive Waste/Department of Energy Spent Nuclear Fuel Short (5–DHLW/DOE SNF Short) co-disposal WP hereinafter termed as "5-DHLW" with emplacement pallet (EP) at room temperature (RT [70°*F* (21°*C*)]) and elevated temperatures for the complete drift collapse event sequence. The repository emplacement drift (RED) collapse will impose a pressure load due to the weight of the rubble rock and thermal expansion due to temperature rise as result of lack of ventilation.

The scope of this calculation is limited to reporting the calculated stress results in terms of the maximum stress intensity (SI) of the WP outer corrosion barrier (OCB) and deformation of the OCB. The stress induced in the OCB is caused by the weight of the loose rock and by self weight of WP components. Time dependency of temperature, material strength and deformation is not considered in this calculation. The cause of the drift collapse is not within the scope of this calculation.

This calculation is intended for use in support of the preliminary design activities for the License Application (LA) design of the WP and is performed by the Thermal/Structural Analysis Discipline.

2. REFERENCES

2.1 PROCEDURES/DIRECTIVES

2.1.1 EG-PRO-3DP-G04B-00037, Rev 9. *Calculations and Analyses*. Las Vegas, Nevada: Bechtel SAIC Company. ACC: ENG.20070717.0004.

2.1.2 IT-PRO-0011, Rev 7, ICN 0. *Software Management.* Las Vegas, NV: Bechtel SAIC Company. ACC: DOC.20070905.0007.

2.1.3 ORD (Office of Repository Development) 2007. *Repository Project Management Automation Plan.* 000-PLN-MGR0-00200-000, Rev. 00E. Las Vegas, Nevada: U.S. Department of Energy, Office of Repository Development. ACC: ENG.20070326.0019.

2.2 DESIGN INPUTS

2.2.1 BSC (Bechtel SAIC Company) 2007. *Basis of Design for the TAD Canister-Based Repository Design Concept.* 000-3DR-MGR0-00300-000-001. Las Vegas, Nevada: Bechtel SAIC Company. ACC: ENG.20071002.0042. ENG.20071026.0033.

2.2.2 BSC (Bechtel SAIC Company) 2007. *TAD Waste Package Configuration.* 000-MW0-DSC0-00101-000 REV 00B. Las Vegas, Nevada: Bechtel SAIC Company. ACC: ENG.20070301.0010.

2.2.3 BSC (Bechtel SAIC Company) 2007. *TAD Waste Package Configuration.* 000-MW0-DSC0-00102-000 REV 00B. Las Vegas, Nevada: Bechtel SAIC Company. ACC:

ENG.20070301.0011.

2.2.4 BSC (Bechtel SAIC Company) 2007. *TAD Waste Package Configuration.* 000-MW0-DSC0-00103-000 REV 00B. Las Vegas, Nevada: Bechtel SAIC Company. ACC: ENG.20070301.0012.

2.2.5 BSC (Bechtel SAIC Company) 2007. *5-DHLW/DOE SNF - Short Co-Disposal Waste Package Configuration.* 000-MW0-DS00-00101-000 REV 00D. Las Vegas, Nevada: Bechtel SAIC Company. ACC: ENG.20070719.0002.

2.2.6 BSC (Bechtel SAIC Company) 2007. *5-DHLW/DOE SNF - Short Co-Disposal Waste Package Configuration.* 000-MW0-DS00-00102-000 REV 00C. Las Vegas, Nevada: Bechtel SAIC Company. ACC: ENG.20070719.0003.

2.2.7 BSC (Bechtel SAIC Company) 2007. *5-DHLW/DOE SNF - Short Co-Disposal Waste Package Configuration.* 000-MW0-DS00-00103-000 REV 00C. Las Vegas, Nevada: Bechtel SAIC Company. ACC: ENG.20070719.0004.

2.2.8 BSC (Bechtel SAIC Company) 2003. *Design and Engineering, Emplacement Pallet Configuration.* 000-M00-TEP0-00101-000-00A. Las Vegas, Nevada: Bechtel SAIC Company. ACC: ENG.20031006.0003.

2.2.9 BSC (Bechtel SAIC Company) 2003. *Design and Engineering, Emplacement Pallet Configuration.* 000-M00-TEP0-00102-000-00A. Las Vegas, Nevada: Bechtel SAIC Company. ACC: ENG.20031006.0004.

2.2.10 BSC (Bechtel SAIC Company) 2003. *Design and Engineering, Emplacement Pallet - Short Configuration.* 000-M00-SSE0-00202-000-00A. Las Vegas, Nevada: Bechtel SAIC Company. ACC: ENG.20031029.0002.

2.2.11 BSC (Bechtel SAIC Company) 2004. *Design and Engineering, Emplacement Pallet Assembly Exploded.* 000-M00-SSE0-00302-000-00A. Las Vegas, Nevada: Bechtel SAIC Company. ACC: ENG.20040224.0006.

2.2.12 BSC (Bechtel SAIC Company) 2004. *Design and Engineering, Emplacement Pallet Waste Package Support Assembly Exploded.* 000-M00-SSE0-00303-000-00A. Las Vegas, Nevada: Bechtel SAIC Company. ACC: ENG.20040224.0007.

2.2.13 BSC (Bechtel SAIC Company) 2004. *Design and Engineering, Emplacement Pallet Assembly Plate 1.* 000-M00-SSE0-00304-000-00A. Las Vegas, Nevada: Bechtel SAIC Company. ACC: ENG.20040224.0008.

2.2.14 BSC (Bechtel SAIC Company) 2004. *Design and Engineering, Emplacement Pallet Assembly Plate 2.* 000-M00-SSE0-00305-000-00A. Las Vegas, Nevada: Bechtel SAIC Company. ACC: ENG.20040224.0009.

2.2.15 BSC (Bechtel SAIC Company) 2004. *Design and Engineering Emplacement Pallet Assembly Plate 3.* 000-M00-SSE0-00306-000-00A. Las Vegas, Nevada: Bechtel SAIC Company. ACC: ENG.20040224.0010.

2.2.16 BSC (Bechtel SAIC Company) 2004. *Design and Engineering, Emplacement Pallet Assembly Plate 4.* 000-M00-SSE0-00307-000-00A. Las Vegas, Nevada: Bechtel SAIC Company. ACC: ENG.20040224.0011.

2.2.17 BSC (Bechtel SAIC Company) 2004. *Design and Engineering, Emplacement Pallet Assembly Plate 5.* 000-M00-SSE0-00308-000-00A. Las Vegas, Nevada: Bechtel SAIC Company. ACC: ENG.20040224.0012.

2.2.18 BSC (Bechtel SAIC Company) 2004. *Design and Engineering, Emplacement Pallet Assembly Plate 6.* 000-M00-SSE0-00309-000-00A. Las Vegas, Nevada: Bechtel SAIC Company. ACC: ENG.20040224.0013.

2.2.19 BSC (Bechtel SAIC Company) 2004. *Design and Engineering, Emplacement Pallet Assembly Plate 7.* 000-M00-SSE0-00310-000-00A. Las Vegas, Nevada: Bechtel SAIC Company. ACC: ENG.20040224.0014.

2.2.20 BSC (Bechtel SAIC Company) 2004. *Design and Engineering, Emplacement Pallet Assembly Plate 8.* 000-M00-SSE0-00311-000-00A. Las Vegas, Nevada: Bechtel SAIC Company. ACC: ENG.20040224.0015.

2.2.21 BSC (Bechtel SAIC Company) 2004. *Design and Engineering, Emplacement Pallet Assembly Plate 9.* 000-M00-SSE0-00312-000-00A. Las Vegas, Nevada: Bechtel SAIC Company. ACC: ENG.20040224.0016.

2.2.22 BSC (Bechtel SAIC Company) 2004. *Design and Engineering, Emplacement Pallet Assembly Tube 1.* 000-M00-SSE0-00313-000-00A. Las Vegas, Nevada: Bechtel SAIC Company. ACC: ENG.20040224.0017.

2.2.23 BSC (Bechtel SAIC Company) 2004. *Design and Engineering, Emplacement Pallet Assembly Tube 2.* 000-M00-SSE0-00314-000-00A. Las Vegas, Nevada: Bechtel SAIC Company. ACC: ENG.20040224.0018.

2.2.24 BSC (Bechtel SAIC Company) 2004. *Design and Engineering, Emplacement Pallet Assembly Tube 3.* 000-M00-SSE0-00315-000-00A. Las Vegas, Nevada: Bechtel SAIC Company. ACC: ENG.20040224.0019.

2.2.25 BSC (Bechtel SAIC Company) 2007. *Waste Package Component Design Methodology Report.* 000-30R-WIS0-00100-000-003. Las Vegas, Nevada: Bechtel SAIC Company. ACC: ENG.20070927.0034; ENG.20071018.0026.

2.2.26 ASME (American Society of Mechanical Engineers) 2001. *2001 ASME Boiler and Pressure Vessel Code (includes 2002 addenda).* New York, New York: American Society of Mechanical Engineers. TIC: 251425.

2.2.27 ASM (American Society for Metals) 1980. *Properties and Selection: Stainless Steels, Tool Materials and Special-Purpose Metals.* Volume 3 of *Metals Handbook.* 9th Edition. Benjamin, D., ed. Metals Park, Ohio: American Society for Metals. TIC: 209801. ISBN: 0-87170-009-3.

2.2.28 Not Used

2.2.29 ASTM G 1-03. 2003. *Standard Practice for Preparing, Cleaning, and Evaluating Corrosion Test Specimens.* West Conshohocken, Pennsylvania: American Society for Testing and Materials. TIC: 259413.

2.2.30 ANSYS V. 8.0. 2004. HP-UX 11.0, HP-UX 11.22, SunOS 5.8. STN: 10364-8.0-00. [DIRS 170070]

2.2.31 DOE (U.S. Department of Energy) 2004. *Validation Test Report for: ANSYS V8.0.* Document Number 10364-VTR-8.0-00. Las Vegas, Nevada: U.S. Department of Energy Office of Repository Development. ACC: MOL.20040422.0376. [DIRS 171758]

2.2.32 LL020603612251.015. Slow Strain Rate Test Generated Stress Corrosion Cracking Data Submittal date: 08/27/2002. [DIRS 160430]

2.2.33 BSC (Bechtel SAIC Company) 2005. *IED Waste Package Processes, Ground Motion Time Histories, and Testing and Materials.* 800-IED-WIS0-00501-000-00A. Las Vegas, Nevada: Bechtel SAIC Company. ACC: ENG.20050406.0004.

2.2.34 BSC (Bechtel SAIC Company) 2004. *Drift Degradation Analysis.* ANL-EBS-MD-000027 REV 03. Las Vegas, Nevada: Bechtel SAIC Company. ACC: DOC.20040915.0010; DOC.20050419.0001; DOC.20051130.0002; DOC.20060731.0005. [DIRS 166107]

2.2.35 MO0408MWDDDMIO.002. Drift Degradation Model Inputs and Outputs. Submittal date: 08/31/2004. [DIRS 171483]

2.2.36 BSC (Bechtel SAIC Company) 2007. *IED Geotechnical and Thermal Parameters III.* 800-IED-MGR0-00403-000-00A. Las Vegas, Nevada: Bechtel SAIC Company. ACC: ENG.20070125.0017; ENG.20070322.0012.

2.2.37 Roark, R.J. and Young, W.C. 1975. *Formulas for Stress and Strain.* 5th Edition. New York, New York: McGraw-Hill. TIC: 240746. ISBN: 0-07-053031-9.

2.2.38 Dieter, G.E. 1976. *Mechanical Metallurgy.* 2nd Edition. Materials Science and Engineering Series. New York, New York: McGraw-Hill Book Company. TIC: 247879. ISBN: 0-07-016891-1.

2.2.39 Boyer, H.E., ed. 2000. *Atlas of Stress-Strain Curves.* Metals Park, Ohio: ASM International. TIC: 248901. ISBN: 0-87170-240-1.

2.2.40 Haynes International. 1997. Hastelloy C-22 Alloy. Kokomo, Indiana: Haynes International. TIC: 238121. ACC: MOL.20021016.0321. [DIRS 100896]

2.2.41 Allegheny Ludlum 2006. Technical Data Blue Sheet, Stainless Steels Chromium-Nickel-Molybdenum, Types 316 (S31600), 316L (S31603), 317 (S31700), 317L (S31703). Technical Data Blue Sheet. [Brackenridge, Pennsylvania]: Allegheny

Ludlum. TIC: 259471. [DIRS 182250]

2.2.42 Avallone, E.A. and Baumeister, T., III, eds. 1987. *Marks' Standard Handbook for Mechanical Engineers.* 9th Edition. New York, New York: McGraw-Hill. TIC: 206891. ISBN: 0-07-004127-X .

2.2.43 BSC (Bechtel SAIC Company) 2007. *Naval Long Waste Package Vertical Impact on Emplacement Pallet and Invert.* 000-00C-DNF0-00100-000-00C. Las Vegas, Nevada: Bechtel SAIC Company. ACC: ENG.20071017.0001.

2.2.44 BSC (Bechtel SAIC Company) 2007. *Waste Package Masses.* 000-00C-MGR0-01100-000-00D. Las Vegas, Nevada: Bechtel SAIC Company. ACC: ENG.20070402.0002.

2.2.45 BSC (Bechtel SAIC Company) 2007. *Drift Cross Section Showing Emplaced Waste Package and Drip Shield.* 800-M00-WIS0-00101-000 REV 00B. Las Vegas, Nevada: Bechtel SAIC Company. ACC: ENG.20070412.0003.

2.2.46 BSC (Bechtel SAIC Company) 2007. *Naval Long Waste Package Configuration.* 000-MW0-DNF0-00101-000 REV 00C. Las Vegas, Nevada: Bechtel SAIC Company. ACC: ENG.20070301.0013.

2.2.47 BSC (Bechtel SAIC Company) 2007. *Naval Long Waste Package Configuration.* 000-MW0-DNF0-00102-000 REV 00C. Las Vegas, Nevada: Bechtel SAIC Company. ACC: ENG.20070301.0014.

2.2.48 BSC (Bechtel SAIC Company) 2007. *Naval Long Waste Package Configuration.* 000-MW0-DNF0-00103-000 REV 00C. Las Vegas, Nevada: Bechtel SAIC Company. ACC: ENG.20070301.0015.

2.3 DESIGN CONSTRAINTS

None

2.4 DESIGN OUTPUTS

The outputs of this report will be used in the following design reports.

2.4.1 BSC 2007. *HLW/DOE SNF Co-Disposal Waste Package Design Report.* 000-00C-DSU0-00600-000, REV 00C. Las Vegas, Nevada: Bechtel SAIC Company.

2.4.2 BSC 2007. *TAD Waste Package Design Report.* 000-00C-DSC0-00100-000, REV 00A. Las Vegas, Nevada: Bechtel SAIC Company.

2.4.3 BSC 2007. *Naval Waste Package Design Report.* 000-00C-DSF0-00800-000, REV 00B. Las Vegas, Nevada: Bechtel SAIC Company.

3. ASSUMPTIONS

3.1 ASSUMPTIONS REQUIRING VERIFICATION

3.1.1 WP and EP Dimensions and Materials

The dimensions, masses, materials, and geometry of the WP and EP used in the development of this calculation correspond to the configuration drawings of References 2.2.2 through 2.2.24, and are assumed to be the same as the final definitive design.

Rationale – The rationale for this assumption is that the designs and drawings of References 2.2.2 through 2.2.24 are created for the LA. This assumption is used in Sections 6.1 and 6.3 and will require verification at completion of the final definitive design.

3.1.2 Applied Pressure on the WP due to Complete Drift Collapse

It is assumed that the pressure load applied on the WP is the same pressure load on the drip shield after a complete collapse of the RED. The magnitude of the applied pressure on the WP OCB after the drift collapse is 403.3 kN/m^2 (kPa) at the top (vertical plane of the WP OCB) and decreases in magnitude radially to 39.6 kPa at the horizontal plane of the WP. The magnitude of the applied pressure is from *Drift Degradation Analysis* (Reference 2.2.34, Table 6-47, Case 2) and *IED Geotechnical and Thermal Parameters III,* Reference 2.2.36, Figure 3.

Rationale – The rationale for this assumption is that the summarized pressure values given in Reference 2.2.34, Table 6-47, are based on a "Continuum Model Analysis" for different drift collapse scenarios, ("Pipe" and "Terzaghi" failure cases) with various "bulking factor". The Continuum Model Analysis approach takes into account the rock mass strength properties and stress state while automatically estimating the ultimate cave shape (Reference 2.2.34, Section 6.4.2.5.3). The "bulking factor" is a factor by which the volume of the rubble increases during cave in process of the RED to fill the tunnel (Reference 2.2.34, Section 6.4.2.5.2.). Case 2 of Reference 2.2.34, Table 6-47 is the largest pressure on the top of the drip shield, 403.3 kPa with a lateral pressure of 39.6 kPa. Applying these values on the WP OCB will give a conservative analysis approach. The source data of Reference 2.2.34, Table 6-47 is given in Reference 2.2.35, and tracked in Reference 2.2.36. A plot of vertical pressure acting on the drip shield as a function of the bulking factor for different failure cases is given in Reference 2.2.34, Figure 6-179, and is tracked in Reference 2.2.36, Figure 3. This assumption will be verified when Table 6-47 of Reference 2.2.34 is included into Reference 2.2.36 (*IED Geotechnical and Thermal Parameters III*). This assumption is used in Sections 6.2 and 6.3.

3.2 ASSUMPTIONS NOT REQUIRING VERIFICATION

3.2.1 RT Poisson's Ratio of Alloy 22

The RT Poisson's ratio of ASME SB-575 [UNS N06022], hereinafter termed as Alloy 22 is not published in traditional sources (such as ASME, ASTM and ASM). Therefore, the RT Poisson's ratio of ASME SB-443 [UNS N06625], hereinafter termed as Alloy 625, is assumed for Alloy 22. The impact of this assumption is anticipated to be negligible.

Rationale – The rationale for this assumption is that the chemical compositions of Alloy 22 and Alloy 625 are similar since they both are 600 Series nickel-base alloys (Reference 2.2.26, Section II, Part B, SB-575, Table 1 and Reference 2.2.27, p. 143 respectively). Therefore, the difference in their Poisson's ratio is expected to be small. Furthermore, there are only small differences in RT Poisson's ratio values for the family of 600 Series nickel-base alloys:

Alloy 600 [UNS N06600] = 0.290 (Reference 2.2.27, p.141)
Alloy 625 [UNS N06625] = 0.278 (Reference 2.2.27, p.143)
Alloy 690 [UNS N06690] = 0.289 (Reference 2.2.27, p.145)

The impact on stress results of small differences in Poisson's ratio is anticipated to be negligible. Stress formulas for cylindrical shells (Reference 2.2.37, Table 30) indicate insensitivity to Poisson's ratio. For the loading case of uniform radial shear loads (Reference 2.2.37, Table 8, Case 8), the key breaching stress, the maximum hoop circumferential membrane stress, is proportional to Poisson's ratio, υ, through the term $(1-\upsilon^2)^{1/4}$. Using the lowest and highest υ values of the three 600 Series nickel-base alloys, 0.278 and 0.290, the difference in maximum hoop circumferential membrane stress values, all parameters assumed constant (being equal) except υ, is a negligible, 0.2%. Therefore, the study of parametric variations provides verification of this assumption per Reference 2.1.1, page 4 ("*Verification may include . . . studies of parametric variations*") and further verification of this assumption is not required. This assumption is used in Section 6.1 and consistent with Section 6.1.1.7 in Reference 2.2.25.

3.2.2 RT Uniform Strain of Alloy 22

The RT uniform strain (engineering strain corresponding to engineering tensile strength) of Alloy 22 is not listed in traditional sources. Therefore, it is assumed that the RT uniform strain is 90% of the RT elongation for Alloy 22.

Rationale – The rationale for this assumption is based on of the shape of RT engineering stress-strain curves for the materials (Reference 2.2.32, S02234_001 Mechanical Deformation, file: "LL020603612251.015 Instron Data Year 2002"). The use of Reference 2.2.32 was approved as the appropriate data for the intended use in an Information Exchange Document (Reference 2.2.33). Therefore this assumption does not require verification. This assumption is used in Section 6.1.2 and corresponds to Section 6.1.1.5 of Reference 2.2.25.

3.2.3 RT Uniform Strain of 316 SS

The RT uniform strain (engineering strain corresponding to engineering tensile strength) of ASME SA-240 [UNS S31600, with modified N & C], hereinafter termed as 316 stainless steel (SS) is not listed in traditional sources. Therefore, it is assumed that the RT uniform strain is 90% of the RT minimum specified elongation for 316 SS.

Rationale – The rationale for this assumption is based on the shape of the stress-strain curve for 316 SS from a qualified source (Reference 2.2.39, p. 304). Therefore this assumption does not require verification. This assumption is used in Section 6.1.2 and corresponds to Section 6.1.1.5 in Reference 2.2.25.

3.2.4 Contact Friction Coefficient

The friction coefficients for contacts occurring between the materials used in this calculation are not published in traditional sources. It is, therefore, assumed that the dynamic (sliding) friction coefficient is 0.4 for all contacts.

Rationale –The rationale for this assumption is that this friction coefficient represents a reasonable lower bound value for most metal-on-metal contacts (see Reference 2.2.42, Table 3.2.1, page 3-26). Sensitivity study performed in Reference 2.2.43, Section 7.3.2 showed that values 0.4 and 1.0 result in the same maximum stress response, using 0.2 results in lower stress response (the sliding surfaces dissipate energy and reduce the impact load). Therefore the assumption of a 0.4 value is reasonable and does not require verification. This assumption is used in Section 6.3 and is consistent with Sections 6.1.1.15 and 6.1.1.16 of Reference 2.2.25.

3.2.5 Elevated Temperature Material Properties

The Poisson's ratio and density at elevated temperatures are not published in traditional sources for Alloy 22 and 316 SS, therefore the RT Poisson's ratio and density are assumed for both Alloy 22 and 316 SS. The impact of using RT Poisson's ratio and density is anticipated to be negligible.

Rationale – The rationale for this assumption is that temperature sensitivities of these material properties are expected to be small and small variations will have negligible affect on the calculation's stress results. Assumption 3.2.1 provides parametric study in this calculation that verifies this (negligible effect of small variations of Poisson's ratio on calculated stress results at RT) for Poisson's ratio of Alloy 22. Assumption 3.2.1 shows how the calculated stress results are not affected by slight variation of Poison's ratio for Alloy 22. The Poisson's ratio values for Alloy 22 and 316 SS at elevated temperature are expected to change slightly from Poisson's ratio values at RT and slight variation is expected to have a negligible effect on the calculated stress results as shown in Assumption 3.2.1. The change in density will be downward as the material expands, inversely related to the volumetric expansion term $(1+\Delta T\alpha)^3$, where ΔT is the temperature increase above RT and α is the relative (to RT) coefficient of thermal expansion. Using $\Delta T = 280°C$ and a clearly upper bound value of 10^{-6} $(°C)^{-1}$ for the materials' α values from 20°C to 300°C, leads to a density change of less than 0.1 %. The total mass will remain unchanged, so the effect of density change on stress is unclear, however even in the unlikely event that the resulting stress effect is a magnitude greater than the density change, it will be negligible. These studies of variations in Poisson's ratio and density provides verification of this assumption per Reference 2.1.1, page 4 *("Verification may include . . . studies of parametric variations")*. Further verification of this assumption is not required. This assumption is used in Section 6.1. This assumption is consistent with Section 6.1.1.11 of Reference 2.2.25.

3.2.6 Minimum Elongation of Alloy 22 and 316 SS at Elevated Temperature

The changes of minimum elongation with an increase of temperature for Alloy 22 and 316 SS are not published in traditional sources. The magnitude of these changes from RT to 600°F (316°C) for Alloy 22 and 316 SS is assumed to be +10% and –30%, respectively, based on the relative changes of typical elongation for these materials available in vendor catalogues (see

Reference 2.2.40, page 15, "Average Tensile Data, Solution Heat-Treated" and Reference 2.2.41, page 8).

Rationale – The rationale for this assumption is that the relative change of minimum elongation with temperature will be reasonably close to the relative change of typical elongation with temperature. Therefore this assumption does not require verification. This assumption is used in Section 6.1 and is consistent with Section 6.1.1.12 of Reference 2.2.25.

3.2.7 TAD and 5–DHLW/DOE SNF Short Co-Disposal WP FEM Simplification

The exact mass and geometry representation of the WP is simplified for the purpose of this calculation. The WP models are represented by the top half-symmetry finite element model (FEM). WP internal components (support ring, spread ring, canister and canister contents) are not included in the FEM. WP components modeled in the finite element representation (FER) are top-half OCB, upper sleeve, OCB top lid, and top-half IV.

Rationale – The rationale for this assumption is that the simplification of the FEM will not affect the output results of the analysis on the OCB. The simplified model will save computation time without affecting the output results of the analysis. The density of the IV is increased so that the total mass of the FER is approximately maintained as given in Reference 2.2.44, Tables 7-1 and 7-5 for TAD and 5-DHLW WPs respectively. Increasing the density of the IV ensures that the total mass is distributed uniformly in the FEM. This is a realistic and equivalent representation of the WP and is done to reduce the overall computation time. This assumption does not require verification and is used in the Section 6.3.

3.2.8 FEM Mesh Verification

TAD WP FEM used for this calculation is the same FEM used in Reference 2.2.43. The FEM mesh used is assumed to be adequate for this analysis and mesh verification is not required. The thicknesses of the OCB and IV of TAD and 5-DHLW WPs are the same and it is assumed that the mesh density used for the TAD WP analysis is sufficient to be used for by the 5-DHLW WP analysis.

Rationale - The rationale for this assumption is that the geometric and material properties of Naval Long WP (Reference 2.2.46 to 2.2.48) and TAD WP (Reference 2.2.2 to 2.2.4) are the same. A mesh verification was performed in Reference 2.2.43, Section 7-1, Table 7-1 for the Naval Long WP, and it shows that the percent change of maximum average shear stress is less one order of magnitude than the percent change of volume for elements with the maximum element wall average (EWA) shear stress for a standard (9 elements across wall thickness) and fine mesh (12 elements across the wall thickness) models. The wall thicknesses of the OCB and IV are the same for TAD and 5-DHLW WPs (Reference 2.2.2 to 2.2.7). The difference in diameter between Naval Long and 5-DHLW WPs will not have any affect on the mesh density across the wall thickness of the OCB and IV. Also, the 5-DHLW FEM was built from the TAD FEM by incorporating the appropriate dimensions and hence the number of nodes and elements in both models are the same. Since the WP length of 5-DHLW is shorter than TAD, the mesh for 5-DHLW model is finer relative to the TAD model. The mesh verification performed in Reference 2.2.43 is consistent with Section 7.1.3 of Reference 2.2.25. Therefore this assumption does not require verification and is used in Section 6.3.

4. METHODOLOGY

4.1 QUALITY ASSURANCE

This calculation was prepared in accordance with EG-PRO-3DP-G04B-00037, *Calculation and Analyses* (Reference 2.1.1). The WP is classified as a safety category item (important to safety and important to waste isolation, ITS/ITWI) (Reference 2.2.1, Section 11.1.2) and the EP is classified as a safety category item (important to waste isolation, ITWI), (Reference 2.2.1, Section 8.1.2). Therefore, the approved version of this document is designated as QA: QA.

4.2 USE OF SOFTWARE

The FEA code used for this calculation is ANSYS V8.0 (Reference 2.2.30). ANSYS V8.0 is identified by the Software Tracking Number (STN) 10364-8.0-00. Usage of ANSYS V8.0 in this calculation constitutes Level 1 software usage, as defined in IT-PRO-0011 (Reference 2.1.2, Attachment 12). ANSYS V8.0 is qualified, baselined, and listed in the current Qualified and Controlled Software Report, as well as the *Repository Project Management Automation Plan* (Reference 2.1.3, Table 6-1).

Computations using ANSYS V8.0 software were executed on Hewlett-Packard (HP) 9000 Series workstations running operating system HP-UX 11.00: The Central processing Unit (CPU) names and their assigned Civilian Radioactive Waste Management System Management and Operating Contractor (CRWMS M&O) tag numbers are listed below;

CPU name: Opus, CRWMS M&O tag number: 151664

CPU name: Milo, CRWMS M&O tag number: 151665

CPU name: Oliver, CRWMS M&O tag number: 150688

CPU name: Rosebud, CRWMS M&O tag number: 150689

CPU name: Portnoy, CRWMS M&O tag number: 150691

The ANSYS V8.0 analyses performed for this calculation are fully within the range of the validation performed for ANSYS V8.0 (Reference 2.2.31). Therefore, ANSYS V8.0 is appropriate for the structural analysis performed in this calculation. Access to, and use of, the code for this calculation is granted by Software Configuration Management in accordance with the appropriate procedures. The details of the ANSYS analyses are described in Section 6.3 and the results are presented in Section 7 of this calculation.

The finite element mesh used in ANSYS finite element analysis, is developed using the commercially available mesh generating software TrueGrid Version 2.3.0 (STN: 610418-2.2.0-00), hereinafter termed as "TrueGrid". TrueGrid is pre-processing software for mesh generation and used solely to mesh geometric representations of the WP and EP for ANSYS simulations and analyses. The suitability and adequacy of the generated mesh is based on visual inspection, engineering judgment, and results of mesh verification (see Assumption 3.2.8). The mesh has been evaluated in accordance with Reference 2.1.1 and determined to be suitable and adequate for use as input to ANSYS. TrueGrid is listed in *Repository Project Management Automation*

Plan (Reference 2.1.3, Table 6-1). TrueGrid usage is Level 2 status as defined in IT-PRO-0011 (Reference 2.1.2, Section 4 and Attachment 12).

Modeling and mesh generation using TrueGrid was executed on the following HP 9000 Series workstations running operating system HP-UX 11.00. The CPU names and their assigned CRWMS M&O tag numbers are listed below;

CPU Name: Opus, CRWMS M&O tag number: 151664

CPU Name: Milo, CRWMS M&O tag number: 151665

CPU Name: Oliver, CRWMS M&O tag number: 150688

CPU Name: Rosebud, CRWMS M&O tag number: 150689

CPU Name: Hodge, CRWMS M&O tag number: 150690

CPU Name: Basselop, CRWMS M&O tag number: 151324

The commercially available Microsoft® Office Excel 2003 (11.8169.8172 SP3) spreadsheet code hereinafter referred to as "Excel", which is a component of Microsoft Office Professional Edition 2003, was used to perform simple calculations. The results of Excel were checked and verified by hand calculations. Usage of Microsoft Office 2003 Professional in this calculation constitutes Level 2 software usage, as defined in IT-PRO-0011 (Reference 2.1.2, Section 4 and Attachment 12). Microsoft Office 2003 Professional is listed in the current controlled Software Report, as well as the *Repository Project Management Automation Plan* (Reference 2.1.3, Table 6-1). Excel was executed on a PC, running Windows XP Professional operating system, Version 5.1.2600, SP 3, Build 2600.

Due to the size of the output (.db) file associated with this calculation, this file created for each simulation has been electronically compressed using commercially available software package. On the HP-UX platform computers the "compress" command is used to compress files, this command comes packaged with the HP-UX 11.00 operating system. The HP-UX platform computer where use of the "compress" command was performed is identified by a CPU name Opus and CRWMS M&O tag number: 151664. The files that were compressed were verified to uncompress correctly by visual inspection. The compressed files have a .Z extension.

4.3 STRESS ANALYSIS APPROACH

FEMs of the WP on the EP are created using TrueGrid and analyzed for RED collapse event using ANSYS. The structural deformation of the WP OCB due to drift collapse (rock) load and WP components self-weight was analyzed to determine any interference between the OCB and the IV components. The WP OCB stress intensity results are reviewed to determine the maximum response locations and magnitudes. The orientation of the WP and EP used in the analyses are based on Reference 2.2.44 without the drip shield.

The design information regarding the WP and EP used in the finite element representation (FER) is based on the existing designs presented in the configuration drawings and sketches of References 2.2.2 through 2.2.24 and Assumptions 3.1.1 and 3.2.7.

The material properties (yield strength, ultimate tensile strength and elongation) used for this calculation are based on ASME B&PV Code (Reference 2.2.26, Section II, Part D, Subpart 1, Table Y-1) minimum strength values. The tangent moduli used for the analysis are calculated using Excel and are listed in the electronic attachment, file: Tangent_Modulus_Calculation.xls, also listed in Section 6.1.3 of this report.

The output peak SI results of the analysis are checked against the ASME allowable SI minimum values listed in Reference 2.2.25, Section 7.1.4, Table 4.

5. LIST OF ATTACHMENTS

Table 5-1. List of Attachments

Attachment	Description	Number of Pages
I	LIST OF FILES ON CD	3
II	CD CONTAINING ELECTRONIC FILES	N/A

6. BODY OF CALCULATION

6.1 MATERIAL PROPERTIES

Material properties used in the calculation of this document are listed in this section. These material properties are used in the design of the WP and EP (see Assumption 3.1.1). Stress units are Pascal (*Pa*), Kilo Pascal ($kPa = 10^3\ Pa$), Mega Pascal ($MPa = 10^6\ Pa$), Giga Pascal ($GPa = 10^9\ Pa$), lb/in^2 (*psi*) and $ksi = 10^3\ psi$.

Alloy 22, (ASME SB-575 [UNS N06022]):- for OCB, Sleeves, and EP

At RT

Density = 8690 kg/m^3 (0.314 lb/in^3)	(Reference 2.2.26, Section II, Part B, SB-575, Section 7.1)
Poisson's ratio = 0.278	(Assumption 3.2.1, see Assumption 3.2.5 for elevated temperatures)
Elongation = 0.45	(Reference 2.2.26, Section II, Part B, SB-575, Table 4)
Yield strength = 310 *MPa* (45 *ksi*)	(Reference 2.2.26, Section II, Part D, Subpart 1, Table Y-1)
Tensile strength = 689 *MPa* (100 *ksi*)	(Reference 2.2.26, Section II, Part D, Subpart 1, Table U)
Modulus of elasticity = 206 *GPa* ($29.9 * 10^6\ psi$)	

Reference 2.2.40, p. 14, vendor supplied data, Table "Average Dynamic Modulus of Elasticity", this data is the best available and suitable for its use in this calculation.

At 300 °F (149 °C)

Yield strength = 254 *MPa* (36.9 *ksi*) (Reference 2.2.26, Section II, Part D, Subpart 1, Table Y-1)

Tensile strength = 679 *MPa* (98.5 *ksi*) (Reference 2.2.26, Section II, Part D, Subpart 1, Table U)

Modulus of elasticity = 198 *GPa* (28.7 * 10^6 *psi*)

Reference 2.2.40, p. 14, vendor supplied data, Table "Average Dynamic Modulus of Elasticity", this data is the best available and suitable for its use in this calculation.

At 600 °F (316 °C)

Yield strength = 211 *MPa* (30.6 *ksi*) (Reference 2.2.26, Section II, Part D, Subpart 1, Table Y-1)

Tensile strength = 628 *MPa* (91.1 *ksi*) (Reference 2.2.26, Section II, Part D, Subpart 1, Table U)

Modulus of elasticity = 191 *GPa* (27.7 * 10^6 *psi*)

Reference 2.2.40, p. 14, vendor supplied data, Table "Average Dynamic Modulus of Elasticity", this data is the best available and suitable for its use in this calculation.

At 1000 °F (538 °C)

Yield strength = 190 *MPa* (27.5 *ksi*) (Reference 2.2.26, Section II, Part D, Subpart 1, Table Y-1)

Tensile strength = 589 *MPa* (85.4 *ksi*) (Reference 2.2.26, Section II, Part D, Subpart 1, Table U)

Modulus of elasticity = 175 *GPa* (25.4 * 10^6 *psi*)

Reference 2.2.40, p. 14, vendor supplied data, Table "Average Dynamic Modulus of Elasticity", this data is the best available and suitable for its use in this calculation.

316 SS, (ASME SA-240 [UNS S31600, with modified N & C]): - For IV, EP Stiffener Tubes

At RT

Density = 7980 *kg/m*^{3} (0.288 *lb/in*^{3}) (Reference 2.2.29, Table X1.1, p. 8)

Poisson's ratio = 0.3 (Reference 2.2.27, Figure 15, p. 755 and see Assumption 3.2.5 for elevated temperatures)

Elongation = 0.40 (Reference 2.2.26, Section II, Part A, SA-240, Table 2)

Yield strength = 207 *MPa* (30 *ksi*) (Reference 2.2.26, Section II, Part D, Subpart 1, Table Y-1)

Tensile strength = 517 *MPa* (75 *ksi*) (Reference 2.2.26, Section II, Part D, Subpart 1, Table U)

Modulus of elasticity = 195 *GPa* (28.3 * 10^6 *psi*) (Reference 2.2.26, Section II, Part D, Subpart 2, Table TM-1)

At 300 °F (149 °C)

Yield strength = 161 *MPa* (23.4 *ksi*) (Reference 2.2.26, Section II, Part D, Subpart 1, Table Y-1)

Tensile strength = 503 *MPa* (72.9 *ksi*) (Reference 2.2.26, Section II, Part D, Subpart 1, Table U)

Modulus of elasticity = 186 *GPa* (27 * 10^6 *psi*) (Reference 2.2.26, Section II, Part D, Subpart 2, Table TM-1)

At 600 °F (316 °C)

Yield strength = 130 *MPa* (18.9 *ksi*) (Reference 2.2.26, Section II, Part D, Subpart 1, Table Y-1)

Tensile strength = 495 *MPa* (71.8 *ksi*) (Reference 2.2.26, Section II, Part D, Subpart 1, Table U)

Modulus of elasticity = 174 *GPa* (25.3 * 10^6 *psi*) (Reference 2.2.26, Section II, Part D, Subpart 2, Table TM-1)

At 1000 °F (538 °C)

Yield strength = 117 *MPa* (17 *ksi*) (Reference 2.2.26, Section II, Part D, Subpart 1, Table Y-1)

Tensile strength = 443 *MPa* (64.3 *ksi*) (Reference 2.2.26, Section II, Part D, Subpart 1, Table U)

Modulus of elasticity = 157 *GPa* (22.8 * 10^6 *psi*) (Reference 2.2.26, Section II, Part D, Subpart 2, Table TM-1)

6.1.1 Calculations for Elevated-Temperature Minimum Elongations

The values for minimum elongation at elevated temperatures are not listed in traditional sources. However, typical elongation values at elevated temperatures are available in vendors' data. The vendor data trends are used to project the minimum RT values from accepted codes to elevated temperatures (see Assumption 3.2.6).

For Alloy 22, the vendor's data shows an approximate 10% relative increase between RT and elevated temperatures, 600°*F* (316°*C*) to 1400°*F* (760°*C*) (Reference 2.2.40, page 15, Table "Average Tensile Data, Solution Heat-Treated"). This data is the best available and suitable for use in this calculation. Therefore, the minimum elongation value for Alloy 22 at elevated temperatures 300°*F* (149°*C*), 600°*F* (316°*C*), and 1000°*F* (538°*C*) is:

$$\text{Minimum elongation} = 0.45 \cdot (1 + 0.1) = 0.50$$

For 316 SS, the vendor's data shows an approximate 30% decrease between RT and 600°F (316°C) (Reference 2.2.41, page 8). This data is the best available and suitable for use in this calculation. Therefore, the minimum elongation values for 316 SS at elevated temperatures 300°F (149°C), 600°F (316°C), and 1000°F (538°C) is (see Assumption 3.2.6):

$$\text{Minimum elongation} = 0.40 \cdot (1 - 0.3) = 0.28$$

6.1.2 Calculations for True Measures of Ductility

The strength properties in Section 6.1 referred to engineering stress and strain definitions (see Reference 2.2.38, Chapter 9):

$$s = \frac{P}{A_0} \text{ and } e = \frac{L - L_0}{L_0}$$

where P stands for the force applied during a static tensile test, L is the deformed-specimen length, and L_0 and A_0 are the original length and cross-sectional area of the specimen, respectively. It is generally accepted that the engineering stress-strain curve does not give a true indication of the deformation characteristics of a material during plastic deformation since it is based entirely on the original dimensions of the specimen. Therefore, the ANSYS finite element code requires input in terms of true stress and true strain definitions:

$$\sigma = \frac{P}{A} \text{ and } \varepsilon = \ln\left(\frac{L}{L_0}\right)$$

The relationships between the true stress and true strain definitions and engineering stress and engineering strain definitions can be readily derived based on constancy of volume ($A_0 \cdot L_0 = A \cdot L$) and strain homogeneity during plastic deformation:

$$\sigma = s \cdot (1 + e) \text{ and } \varepsilon = \ln(1 + e)$$

These expressions are applicable only in the hardening region of the stress-strain curve before the onset of necking (before stresses reach the tensile strength).

The following parameters are used in the subsequent calculations:

$s_y \approx \sigma_y$ = yield strength

s_u = engineering tensile strength

σ_u = true tensile strength

$e_y \approx \varepsilon_y$ = strain corresponding to tensile yield strength

e_u = engineering strain corresponding to engineering tensile strength (uniform strain)

ε_u = true strain corresponding to true tensile strength (true uniform strain)

Uniform strain data are not listed in traditional sources and it needs to be estimated based on stress-strain curves and the minimum specified elongation. For Alloy 22 and 316 SS, the

minimum elongation, reduced by 10% is used for the uniform strain (see Assumptions 3.2.2 and 3.2.3).

In absence of data on the uniform strain in traditional sources, the uniform strain needs to be estimated based on the character of stress-strain curves and elongation (strain corresponding to rupture of the tensile specimen).

Note: All the calculated values are from Excel spreadsheet (Attachment-II, file: Tangent_Modulus_Calculation.xls)

Alloy 22: (see Attachment –II, file: Tangent_Modulus_Calculation.xls)

$e_u = 0.9 \cdot elongation = 0.9 \cdot 0.45 = 0.41$ at RT

$e_u = 0.9 \cdot 0.5 = 0.45$ at 300°*F* (149°*C*), 600°*F* (316°*C*) and 1000°*F* (538°*C*)

$\varepsilon_u = \ln(1 + e_u) = \ln(1 + 0.41) = 0.34$ at RT

$\varepsilon_u = \ln(1 + e_u) = \ln(1 + 0.45) = 0.37$ at 300°*F* (149°*C*), 600°*F* (316°*C*) and 1000°*F* (538°*C*)

$\sigma_u = s_u \cdot (1 + e_u) = 689 \cdot (1 + 0.41) = 968$ *MPa* (140.36 *ksi*) at RT

$\sigma_u = s_u \cdot (1 + e_u) = 679 \cdot (1 + 0.45) = 981$ *MPa* (142.25 *ksi*) at 300°*F* (149°*C*)

$\sigma_u = s_u \cdot (1 + e_u) = 628 \cdot (1 + 0.45) = 908$ *MPa* (131.66 *ksi*) at 600°*F* (316°*C*)

$\sigma_u = s_u \cdot (1 + e_u) = 589 \cdot (1 + 0.45) = 851$ *MPa* (123.40 *ksi*) at 1000°*F* (538°*C*)

316 SS: (see Attachment-II, file: Tangent_Modulus_Calculation.xls)

$e_u = 0.9 \cdot elongation = 0.9 \cdot 0.40 = 0.36$ at RT

$e_u = 0.9 \cdot 0.28 = 0.25$ at 300°*F* (149°*C*), 600°*F* (316°*C*) and 1000°*F* (538°*C*)

$\varepsilon_u = \ln(1 + e_u) = \ln(1 + 0.36) = 0.31$ at RT

$\varepsilon_u = \ln(1 + e_u) = \ln(1 + 0.25) = 0.22$ at 300°*F* (149°*C*), 600°*F* (316°*C*) and 1000°*F* (538°*C*)

$\sigma_u = s_u \cdot (1 + e_u) = 517 \cdot (1 + 0.36) = 703$ *MPa* (101.94 *ksi*) at RT

$\sigma_u = s_u \cdot (1 + e_u) = 503 \cdot (1 + 0.25) = 630$ *MPa* (91.35 *ksi*) at 300°*F* (149°*C*)

$\sigma_u = s_u \cdot (1 + e_u) = 495 \cdot (1 + 0.25) = 620$ *MPa* (89.9 *ksi*) at 600°*F* (316°*C*)

$\sigma_u = s_u \cdot (1 + e_u) = 443 \cdot (1 + 0.25) = 555$ *MPa* (80.48 *ksi*) at 1000°*F* (538°*C*)

6.1.3 Calculations for Tangent Moduli

When metals are driven into the plastic range, the slope of the stress-strain curve continuously changes. A simplification of this curve is used to incorporate plasticity into the FERs. A standard post-yield approximation commonly used in engineering is to use a straight line between the yield point and the ultimate tensile strength point of the material (bilinear elasto-plastic representation).

ANSYS solutions are performed using true stress and true strain. Therefore, a bilinear true stress – true strain curve is constructed. The only new parameter in the subsequent calculations is the tangent (hardening) modulus (E_1), the plastic region slope of this bilinear true stress – true strain curve.

RT corresponding strain and tangent modulus for Alloy 22 are:

Strain,

$$\varepsilon_y = \sigma_y / E = 310 \cdot 10^6 \, Pa / 206 \cdot 10^9 \, Pa = 1.5 \cdot 10^{-3}$$

Tangent modulus,

$$E_1 = (\sigma_u - \sigma_y) / (\varepsilon_u - \varepsilon_y) = (0.968 - 0.310) GPa / (0.34 - 1.5 \cdot 10^{-3}) = 1.94 \ GPa \ (281.3 \ ksi)$$

An elevated temperature corresponding strain and tangent modulus for Alloy 22 are:

At 300°*F* (149°*C*)

Strain,

$$\varepsilon_y = \sigma_y / E = 254 \cdot 10^6 \, Pa / 198 \cdot 10^9 \, Pa = 1.28 \cdot 10^{-3}$$

The tangent modulus,

$$E_1 = (\sigma_u - \sigma_y) / (\varepsilon_u - \varepsilon_y) = (0.981 - 0.254) GPa / (0.37 - 1.28 \cdot 10^{-3}) = 1.98 \ GPa \ (287.1 \ ksi)$$

At 600°*F* (316°*C*)

Strain,

$$\varepsilon_y = \sigma_y / E = 211 \cdot 10^6 \, Pa / 191 \cdot 10^9 \, Pa = 1.1 \cdot 10^{-3}$$

Tangent modulus,

$$E_1 = (\sigma_u - \sigma_y) / (\varepsilon_u - \varepsilon_y) = (0.908 - 0.211) GPa / (0.37 - 1.1 \cdot 10^{-3}) = 1.90 \ GPa \ (275.5 \ ksi)$$

At 1000°*F* (538°*C*)

Strain,

$$\varepsilon_y = \sigma_y / E = 190 \cdot 10^6 \, Pa / 175 \cdot 10^9 \, Pa = 1.09 \cdot 10^{-3}$$

Tangent modulus,

$$E_1 = (\sigma_u - \sigma_y) / (\varepsilon_u - \varepsilon_y) = (0.851 - 0.19) GPa / (0.37 - 1.09 \cdot 10^{-3}) = 1.80 \ GPa \ (261 \ ksi)$$

316 SS with modified carbon and nitrogen

RT corresponding strain and tangent modulus of 316 SS are:

Strain,

$$\varepsilon_y = \sigma_y / E = 207 \cdot 10^6 \, Pa / 195 \cdot 10^9 \, Pa = 1.06 \cdot 10^{-3}$$

Tangent modulus,

$$E_1 = (\sigma_u - \sigma_y)/(\varepsilon_u - \varepsilon_y) = (0.703 - 0.207)GPa/(0.31 - 1.06 \cdot 10^{-3}) = 1.62\ GPa\ (234.9\ ksi)$$

An elevated temperature corresponding strain and tangent modulus of 316 SS are:

At 300°F (149°C)

Strain,

$$\varepsilon_y = \sigma_y / E = 161 \cdot 10^6\ Pa / 186 \cdot 10^9\ Pa = 0.86 \cdot 10^{-3}$$

Tangent modulus,

$$E_1 = (\sigma_u - \sigma_y)/(\varepsilon_u - \varepsilon_y) = (0.630 - 0.161)GPa/(0.22 - 0.86 \cdot 10^{-3}) = 2.09\ GPa\ (303.05\ ksi)$$

At 600°F (316°C)

Strain

$$\varepsilon_y = \sigma_y / E = 130 \cdot 10^6\ Pa / 174 \cdot 10^9\ Pa = 0.747 \cdot 10^{-3}$$

Tangent modulus

$$E_1 = (\sigma_u - \sigma_y)/(\varepsilon_u - \varepsilon_y) = (0.620 - 0.130)GPa/(0.22 - 0.747 \cdot 10^{-3}) = 2.19\ GPa\ (317.55\ ksi)$$

At 1000°F (538°C)

Strain

$$\varepsilon_y = \sigma_y / E = 117 \cdot 10^6\ Pa / 157 \cdot 10^9\ Pa = 0.745 \cdot 10^{-3}$$

The tangent modulus is

$$E_1 = (\sigma_u - \sigma_y)/(\varepsilon_u - \varepsilon_y) = (0.555 - 0.117)GPa/(0.22 - 0.745 \cdot 10^{-3}) = 1.95\ GPa\ (282.75\ ksi)$$

6.2 APPLIED PRESSURE ON THE WP

Drift collapse can occur either in the preclosure or postclosure periods. For this document a preclosure drift collapse scenario is considered. In the preclosure drift collapse scenario, the drip shields are not yet placed in the drift, therefore the rock rubble falls directly onto the emplaced WP rested on the EP. The pressure load acting on the drip shield after a complete drift collapse is applied directly onto the WP (see Assumption 3.1.2). The magnitude of the applied pressure is based on Reference 2.2.34, Table 6-47, Case 2, with a maximum value of 403.3 *kPa* at the top (vertical plane of the WP) and reduce in magnitude radially to 39.6 *kPa* along the horizontal plane of the WP. Of "Piping" and 'Terzaghi" failure types the former induces the maximum vertical pressure and "Piping" failure case is used for this calculation (Reference 2.2.34, Table 6-47, Case2).

6.3 FINITE ELEMENT REPRESENTATION

The FER of TAD WP while rested on the EP with applied pressure load, boundary conditions and gravity load is shown in Figures 6-1 and 6-2. An isometric view of TAD WP FER is shown in Figure 6-3. An outlined representation of the TAD WP is given in Figure 6-4. The FER of 5-DHLW WP while rested on the EP with applied pressure load, boundary conditions and gravity load is shown in Figures 6-5 and 6-6. An isometric view of 5-DHLW WP FER is shown in Figure 6-7. An outlined representation of the 5-DHLW WP is shown Figure 6-8. The FER of the WP is simplified to reduce computation time without compromising the structural response. The total mass of the half-symmetry WP FEM is maintained by increasing the density of the IV (see Assumption 3.2.7). Hence, the IV density used in the analysis is higher than the density of 316 SS in Section 6.1. The upper end of the WP is represented in the FEM. FERs are developed by using dimensions and geometric properties provided in References 2.2.2 through 2.2.24 and Assumptions 3.1.1, 3.2.7, and 3.2.8. The pressure loads used in the FER are provided in Assumption 3.1.2 and Section 6.2. Material properties of the FER at RT and elevated temperatures are given in Section 6.1 with modified IV density.

A standard mesh with 9 elements through the wall thickness of the OCB was used for the analysis. Mesh verification was not performed in this calculation since the FEM is from a previous calculation, Reference 2.2.43 (See Assumption 3.2.8).

A static and sliding friction coefficient of 0.4 was used for all contact surfaces between WP components and EP (see Assumption 3.2.4).

The orientation of the WP and the EP at different temperatures analyses cases was based on Reference 2.2.44. The gap between all contacting surfaces is closed before the analysis, IV outer surface is in direct contact with the OCB inner surface and the OCB outer surface is in contact with the EP. The analysis of "no-gap" orientation is simulated with different temperature material properties.

An elastic-plastic structural finite element analysis was performed on the FER using the commercially available ANSYS V.8.0 finite element code (Reference 2.2.30). Two WP configurations for the LA (see Assumption 3.1.1) were investigated at RT and elevated temperatures, 300°*F* (149°*C*), 600°*F* (316°*C*) and 1000°*F* (538°*C*) to determine WP OCB structural response to the complete drift collapse event sequence. Since the maximum deflection of the OCB (9.63 *mm* at 1000°*F* for TAD WP) is less than 50% of the OCB wall thickness (1 *in* [25.4 *mm*]), non-linear geometry effects were not considered in the FEA. The peak SI of the FEM is compared against the minimum ASME Code allowable SI as summarized in Reference 2.2.25, Table 4.

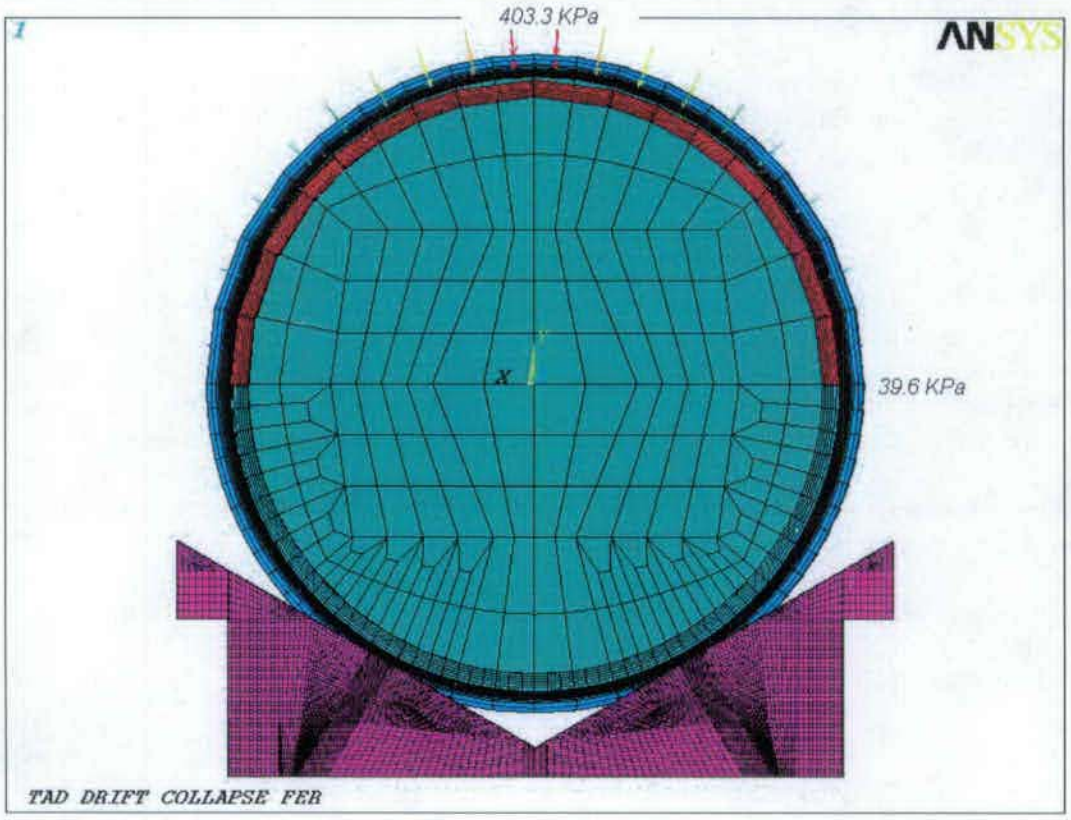

Figure 6-1. FEM of the TAD WP rested on EP showing Applied Pressure Loads

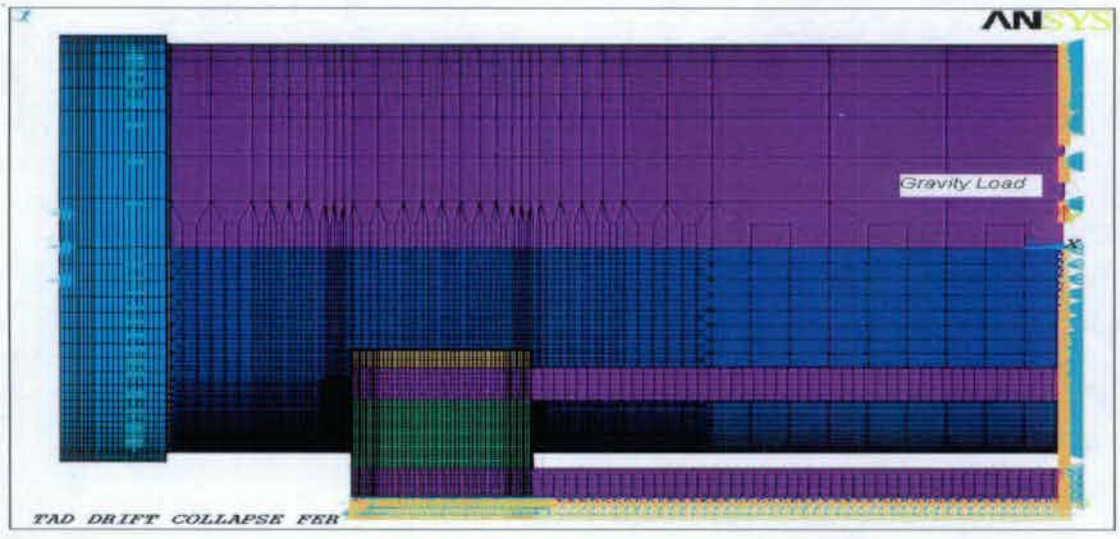

Figure 6-2. FER of TAD WP rested on EP with Boundary Conditions and Gravity Load

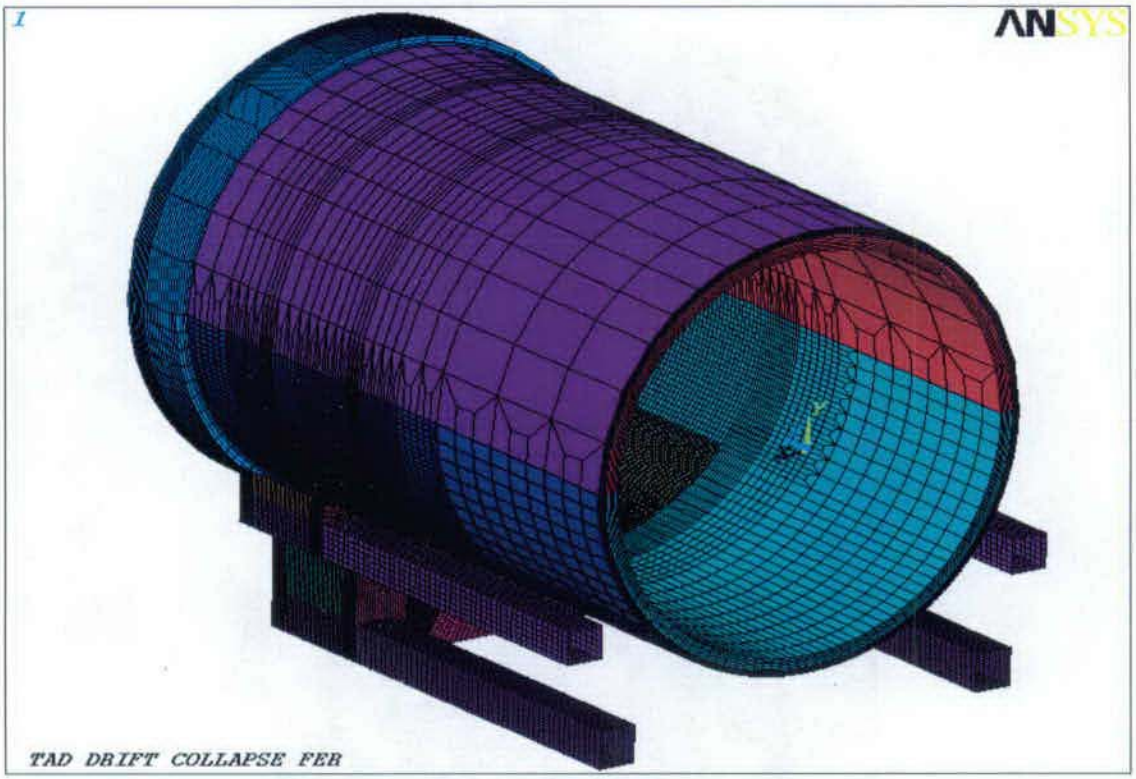

Figure 6-3. FEM of the TAD WP rested on EP (Isometric View)

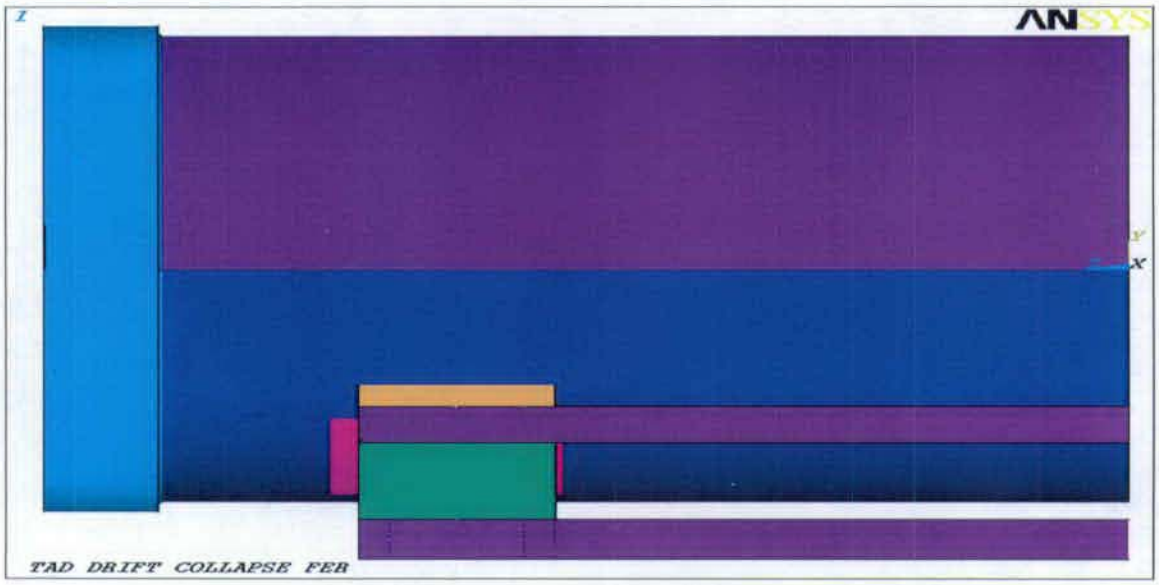

Figure 6-4. Outline Model of the TAD WP rested on EP (Side View)

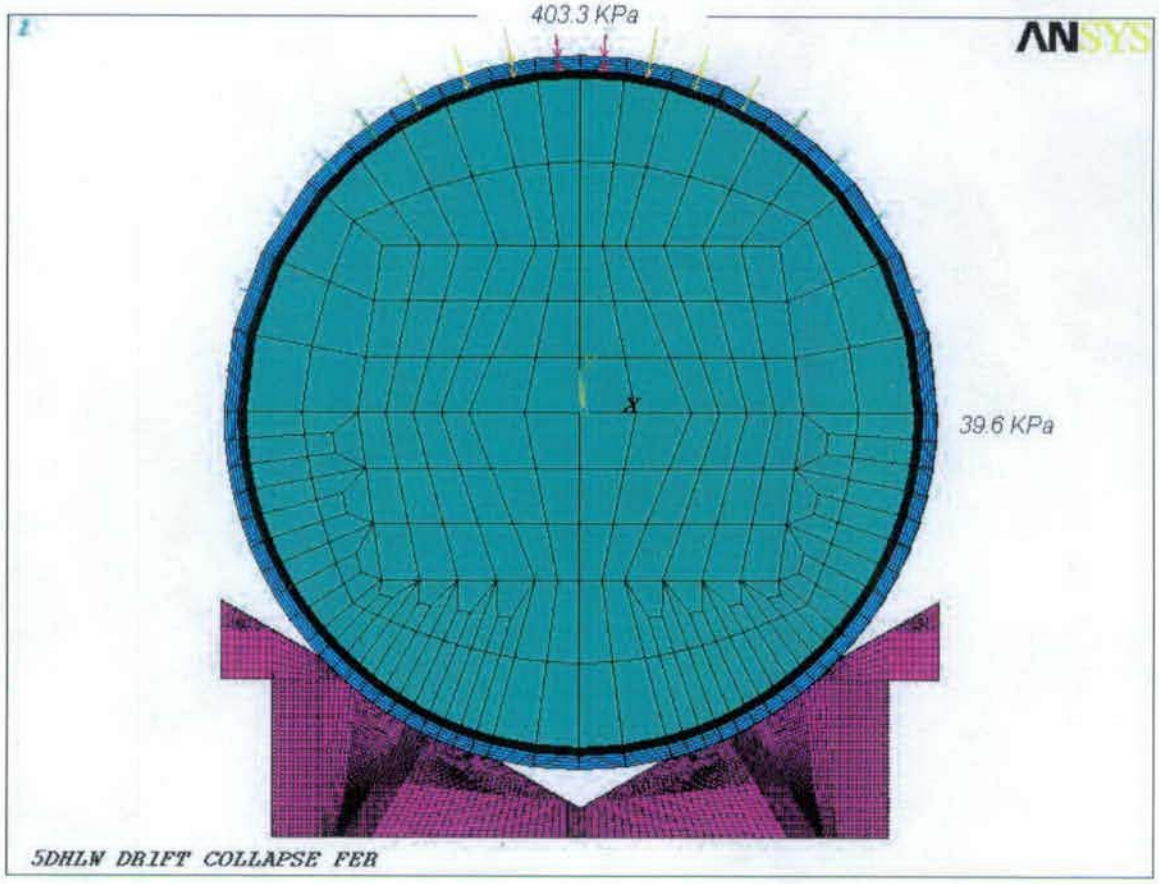

Figure 6-5. FEM of the 5-DHLW WP rested on EP showing Applied Pressure Loads

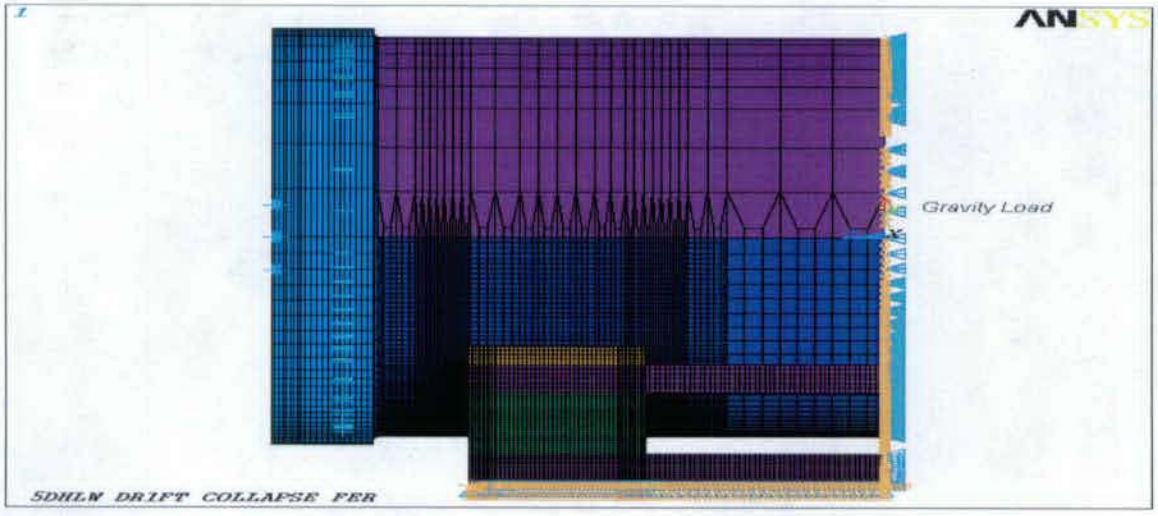

Figure 6-6. FEM of the 5-DHLW WP with Boundary Conditions & Gravity Load

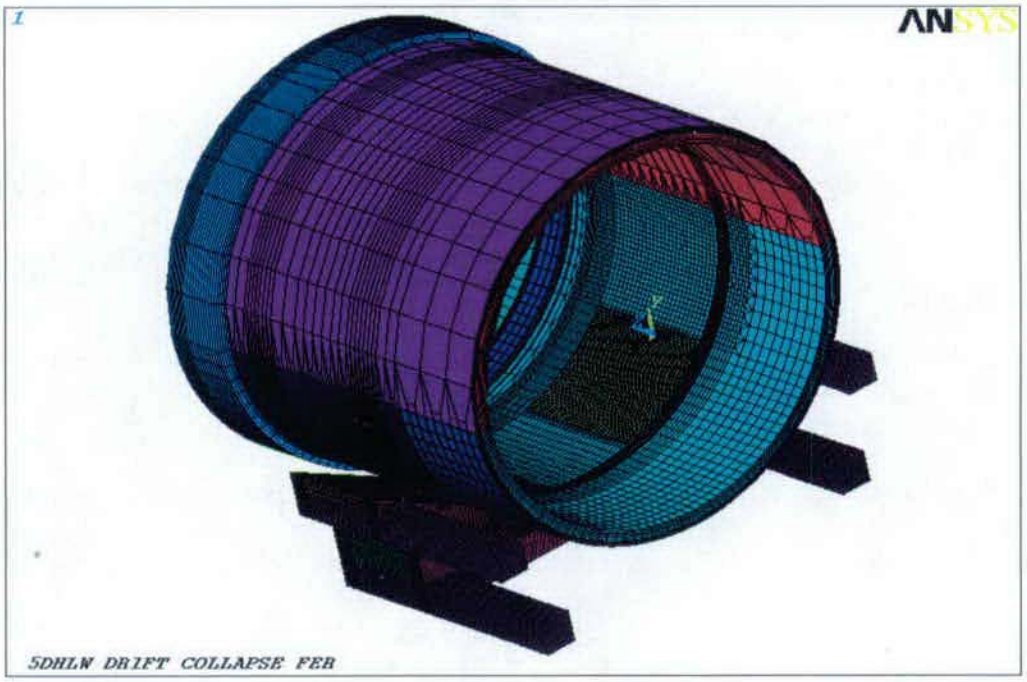

Figure 6-7. FEM of the 5-DHLW WP rested on EP (Isometric View)

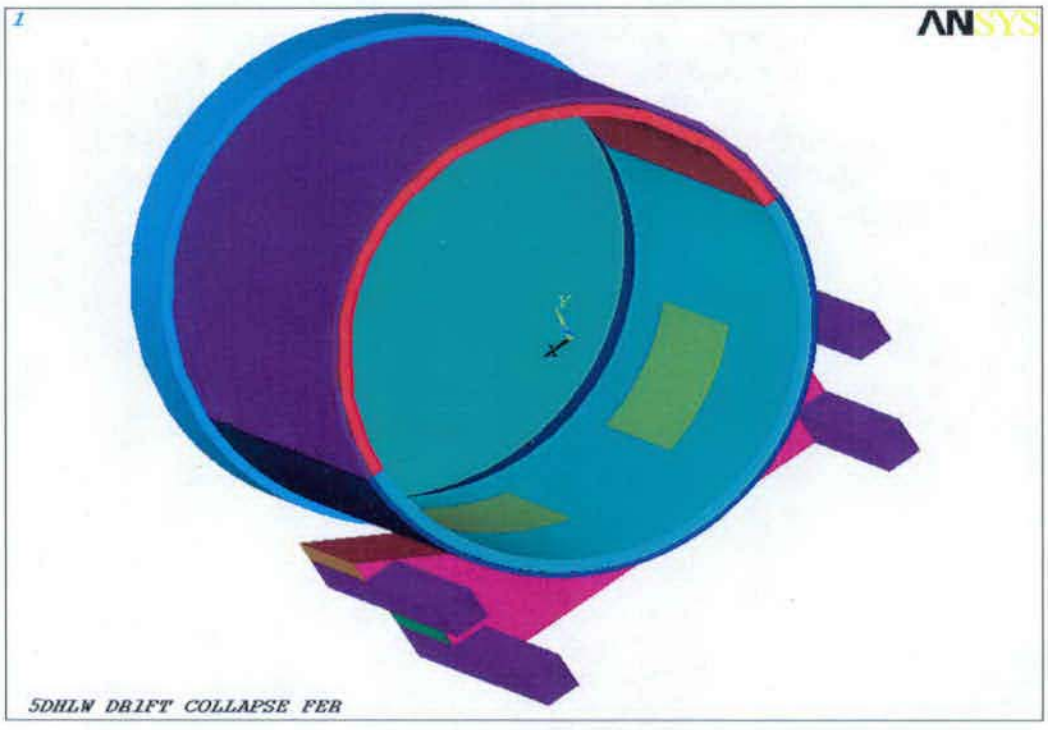

Figure 6-8. Outline Model of the 5-DHLW WP rested on EP (Isometric View)

7. RESULTS AND CONCLUSIONS

Attachment II (electronic CD) includes the compressed database (.db.Z), monitor (.mntr), TrueGrid (.tg), and Nodes_SI & Nodes_DY output text (.txt) files that show execution of the successful simulations. It also includes the file that contains the modified density calculations of the IV and mass verification of the two analyzed WPs. The FER mass output text files from TrueGrid converted into Excel file, lists the FER masses for TAD and 5DHLW WPs in separate worksheets labeled appropriately. As seen, the difference between the actual (Reference 2.2.44, Tables 7-1 and 7-5) and simulated masses for both WPs is negligible.

Figures 7-1 to 7-16 show the stress intensity and displacement contour plots inclusive of peak values for RT and elevated temperature cases. Maximum stresses are found at the OCB outer surface in the vicinity of contact between the OCB and EP resting plates.

The results obtained from ANSYS are reported in terms of average nodal maximum SI and displacements. Stress intensity (see Reference 2.2.26, Section III, Division 1, Appendix XIII, XIII-1123(a)) is defined as the difference between maximum and minimum principal stress.

The maximum stress intensities are found at the end of the simulation when all loads have been fully applied. Table 7-1 shows the peak stress intensities in the OCB at different temperatures considered in this calculation for both the TAD and 5DHLW WPs. Table 7-1 also lists the ratios of peak stress intensity to true tensile strength. It must be noted that since the peak stress values are well below the limit of $0.7\sigma_u$, wall-averaging of stresses through the wall thickness of the OCB is not needed. TAD WP loaded at RT shows the peak stress of 365 *MPa* (see Figure 7-1). Table 7-2 shows the peak displacement in the OCB at the different temperatures considered in this calculation for both the TAD and 5DHLW WPs. TAD WP loaded at $1000^{o}F$ shows the peak displacement of 9.63 *mm* (see Figure 7-8). It must be noted that the IV is modeled without the lid and internals, and has not been studied in this calculation. The total mass of the FER is maintained as given in Reference 2.2.44, Tables 7-1 and 7-5 for TAD and 5-DHLW WPs respectively by increasing the density of the IV (see Attachment II, CD file: Mass_Verification.xls).

Table 7-1. Maximum Stress Intensity [*MPa*] on the OCB

Run #	WP	Temperature	Figure #	Node # on OCB	σ_u (*MPa*)	Peak SI (*MPa*) on OCB	SI/σ_u
1A	TAD	RT	7-1	63265	968	365	0.377
2A	TAD	300°*F*	7-3	60214	981	300	0.306
3A	TAD	600°*F*	7-5	60214	908	257	0.283
4A	TAD	1000°*F*	7-7	60214	851	240	0.282
1B	5DHLW	RT	7-9	170381	968	359	0.371
2B	5DHLW	300°*F*	7-11	120892	981	300	0.306
3B	5DHLW	600°*F*	7-13	120890	908	260	0.286
4B	5DHLW	1000°*F*	7-15	90489	851	222	0.261

Table 7-2. Maximum Displacement [*mm*] of the OCB

Run #	WP	Temperature	Figure #	Node # on OCB	Peak Displacement *mm*)
1A	TAD	RT	7-2	239540	7.99
2A	TAD	300°*F*	7-4	239540	8.36
3A	TAD	600°*F*	7-6	239540	8.78
4A	TAD	1000°*F*	7-8	239540	9.63
1B	5DHLW	RT	7-10	239524	3.67
2B	5DHLW	300°*F*	7-12	239524	3.79
3B	5DHLW	600°*F*	7-14	239524	3.94
4B	5DHLW	1000°*F*	7-16	239524	4.27

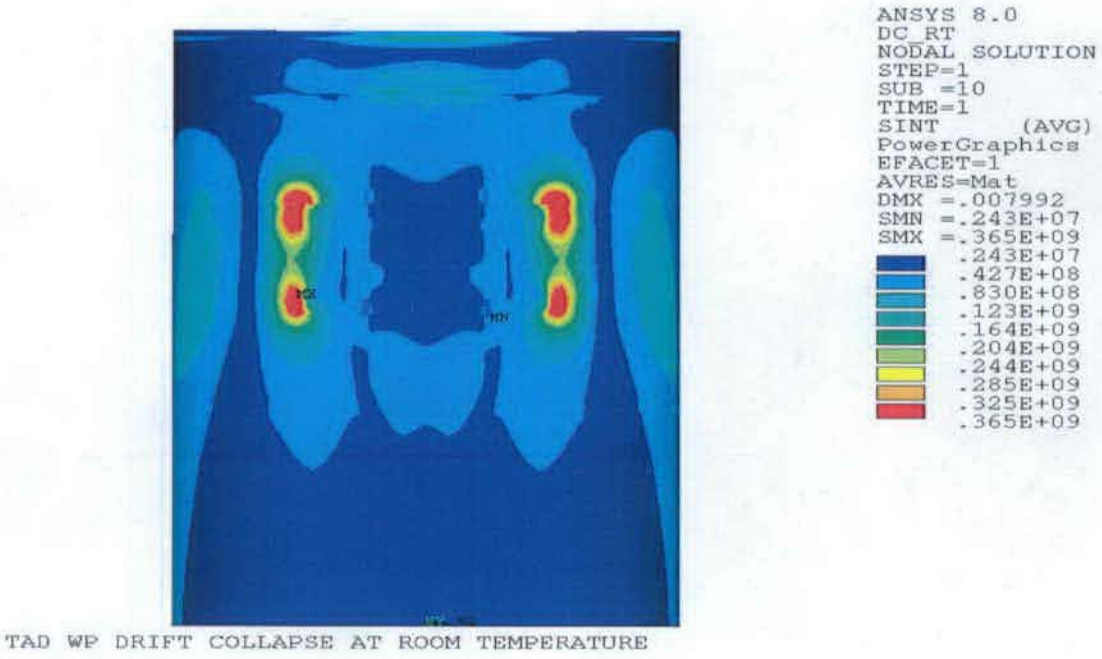

Figure 7-1. TAD OCB Peak Stress Intensity [*GPa*] Contour Plot (Run 1A)

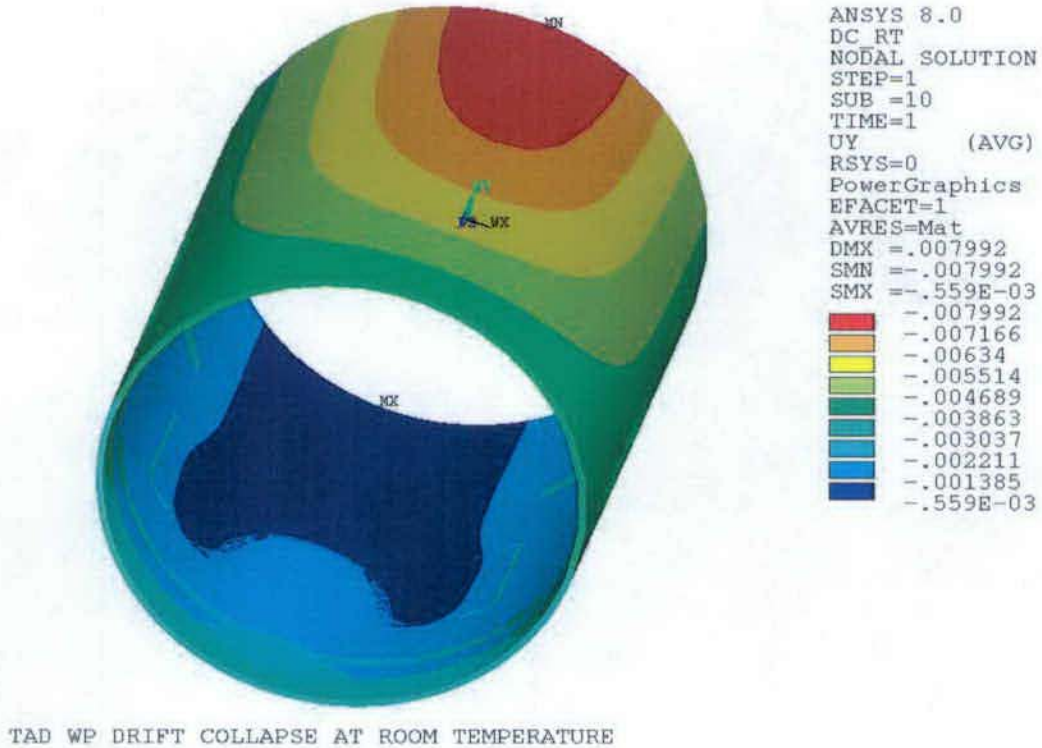

Figure 7-2. TAD OCB Peak Displacement [*m*] Contour Plot (Run 1A)

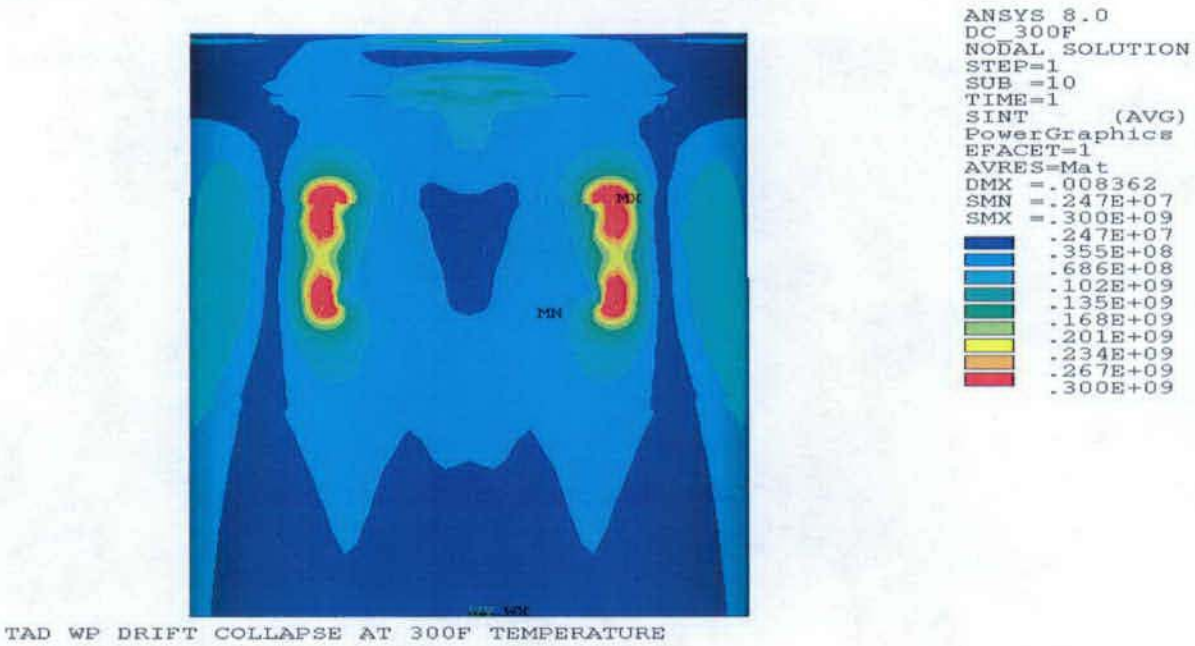

Figure 7-3. TAD OCB Peak Stress Intensity [*GPa*] Contour Plot (Run 2A)

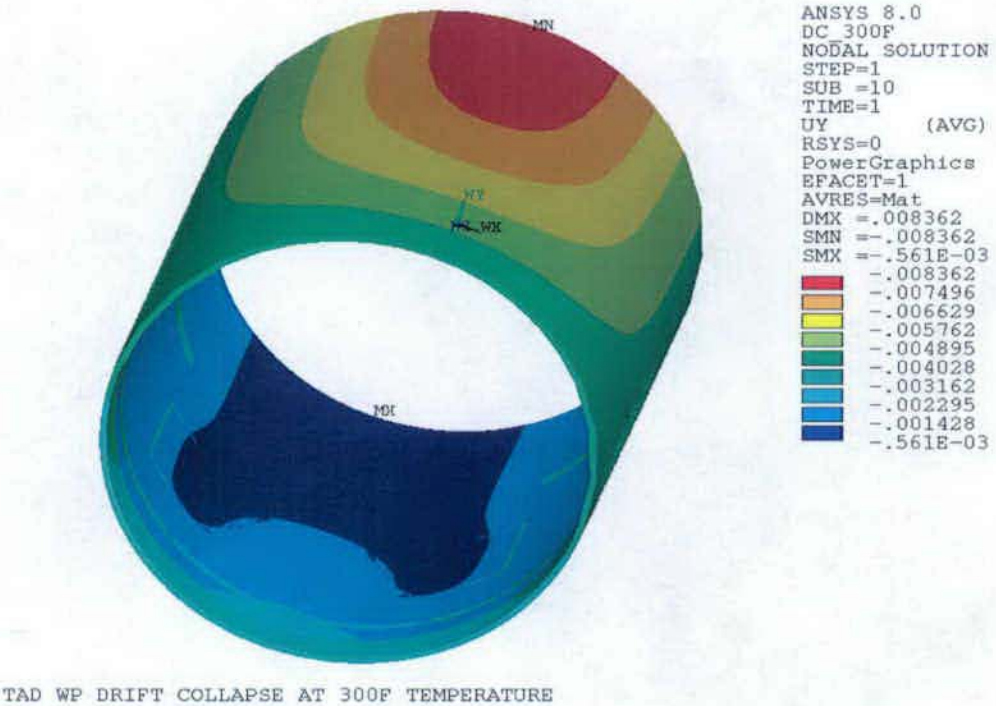

Figure 7-4. TAD OCB Peak Displacement [*m*] Contour Plot (Run 2A)

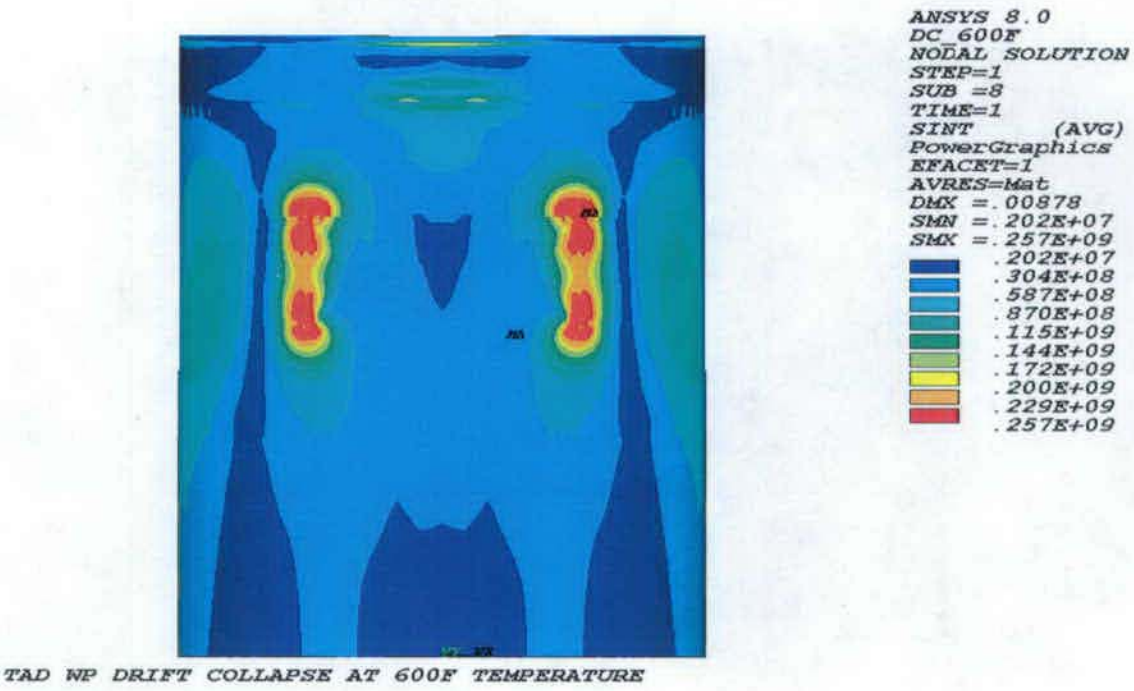

Figure 7-5. TAD OCB Peak Stress Intensity [*GPa*] Contour Plot (Run 3A)

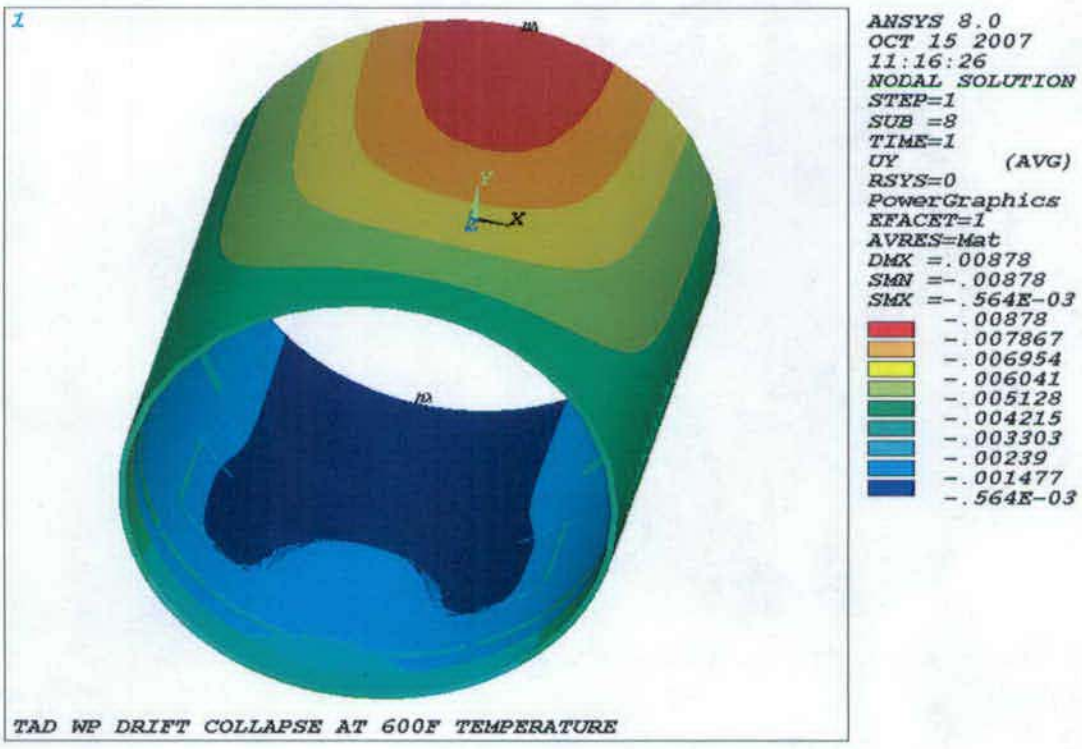

Figure 7-6. TAD OCB Peak Displacement [*m*] Contour Plot (Run 3A)

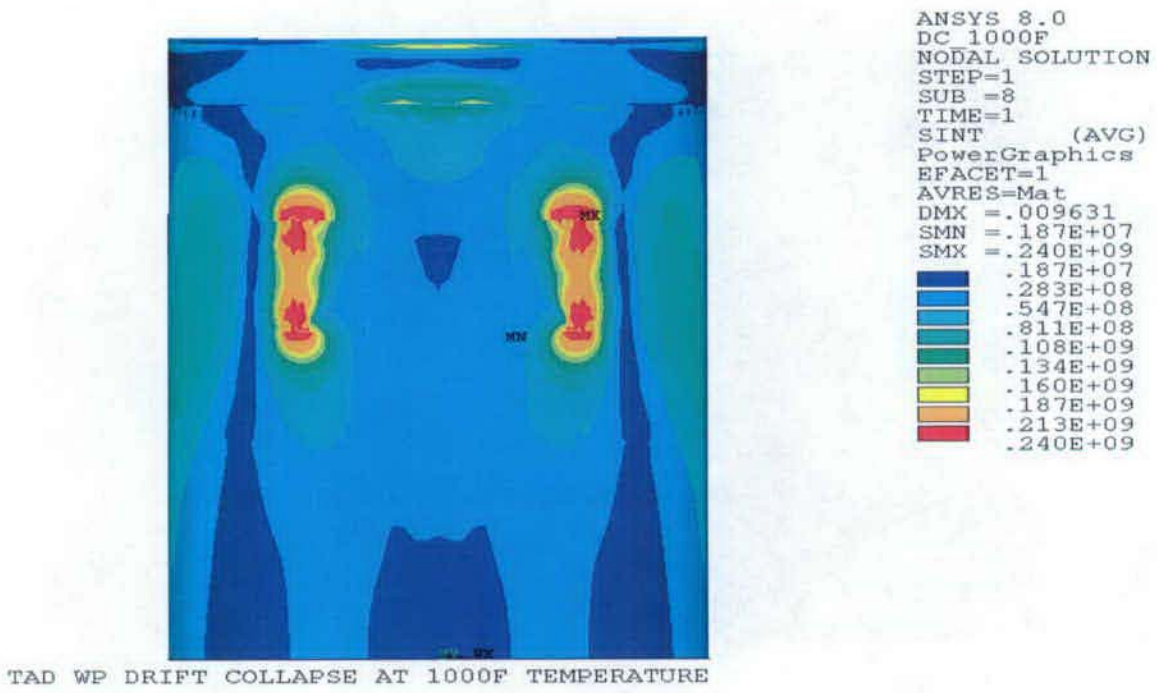

Figure 7-7. TAD OCB Peak Stress Intensity [*GPa*] Contour Plot (Run 4A)

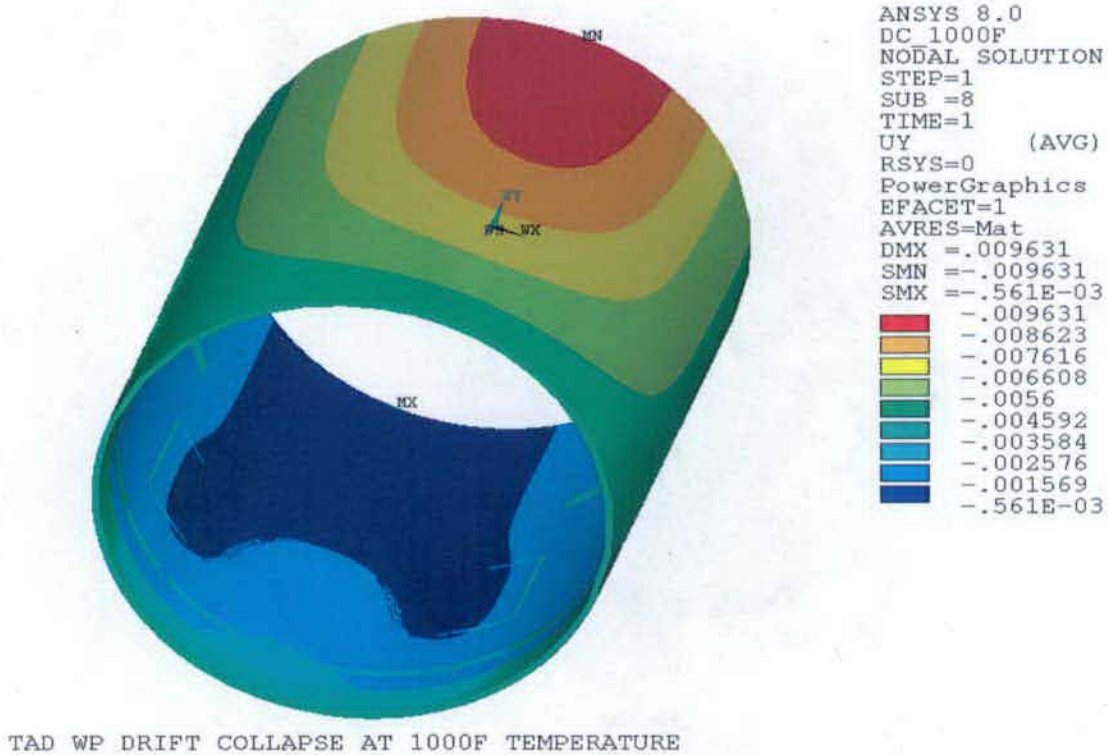

Figure 7-8. TAD OCB Peak Displacement [*m*] Contour Plot (Run 4A)

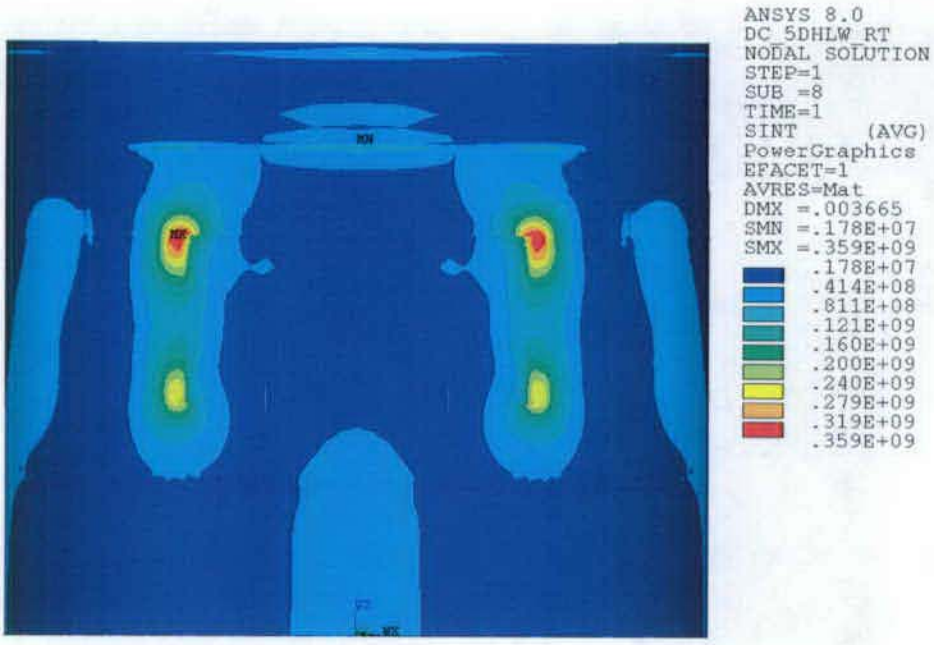

Figure 7-9. 5-DHLW OCB Peak Stress Intensity [*GPa*] Contour Plot (Run 1B)

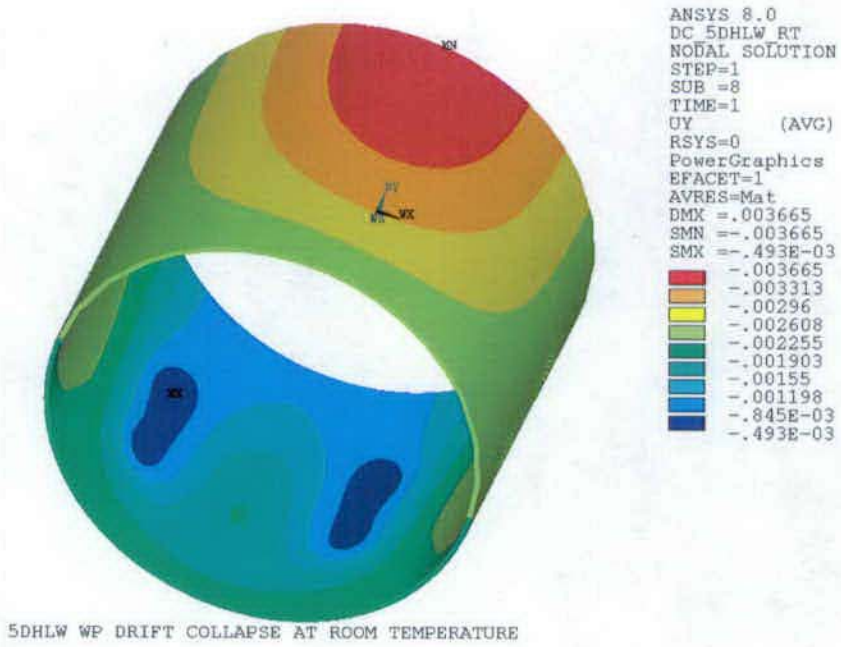

Figure 7-10. 5-DHLW OCB Peak Displacement [*m*] Contour Plot (Run 1B)

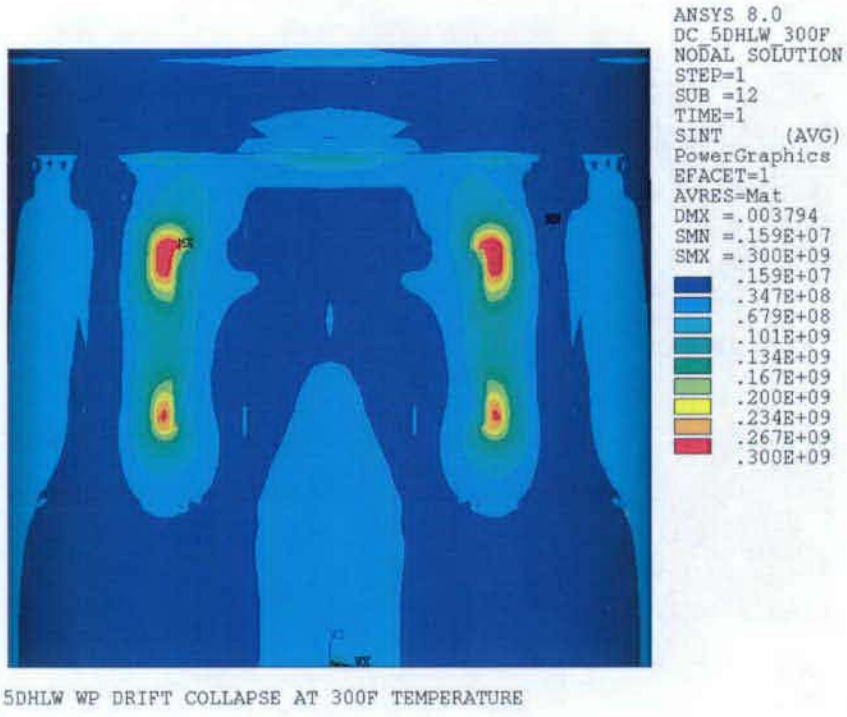

Figure 7-11. 5-DHLW OCB Peak Stress Intensity [*GPa*] Contour Plot (Run 2B)

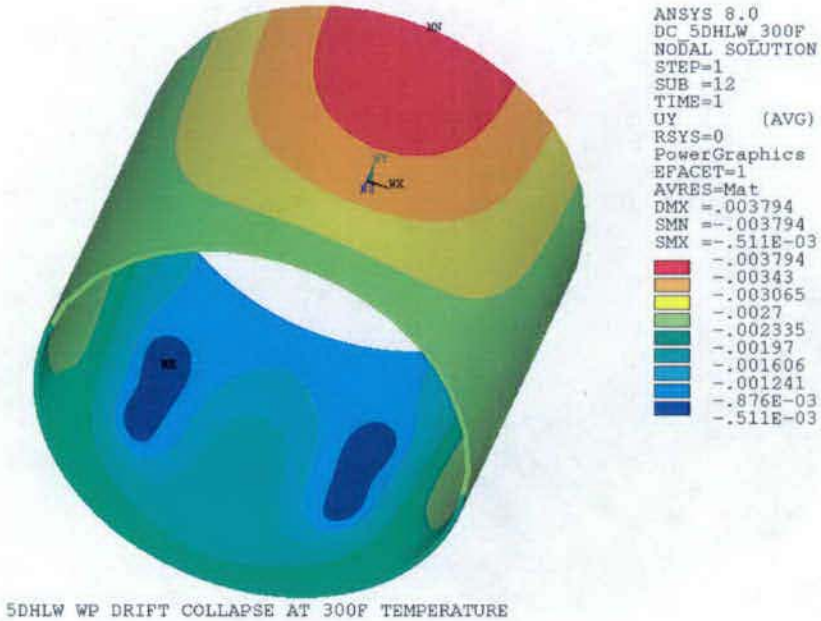

Figure 7-12. 5-DHLW OCB Peak Displacement [*m*] Contour Plot (Run 2B)

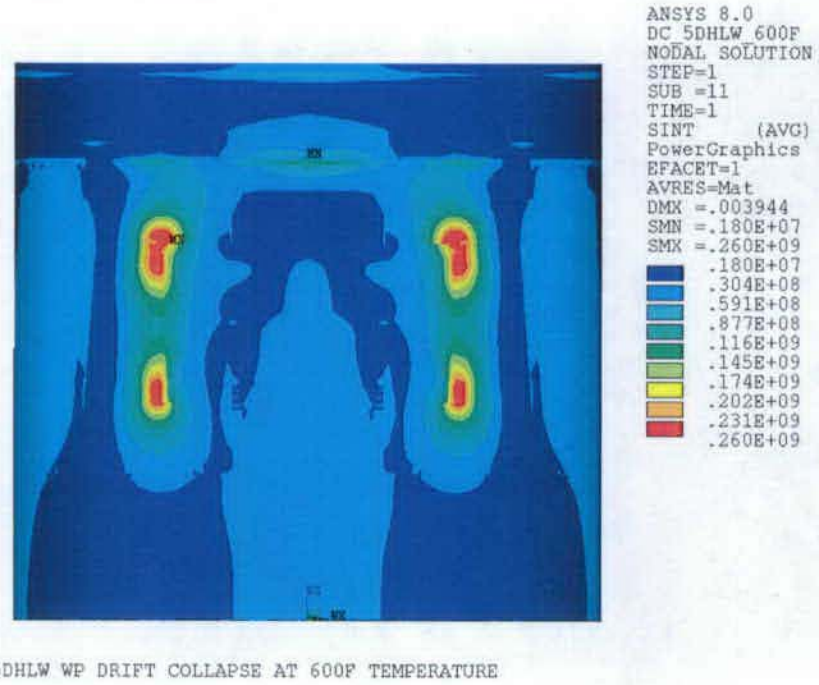

Figure 7-13. 5-DHLW OCB Peak Stress Intensity [*GPa*] Contour Plot (Run 3B)

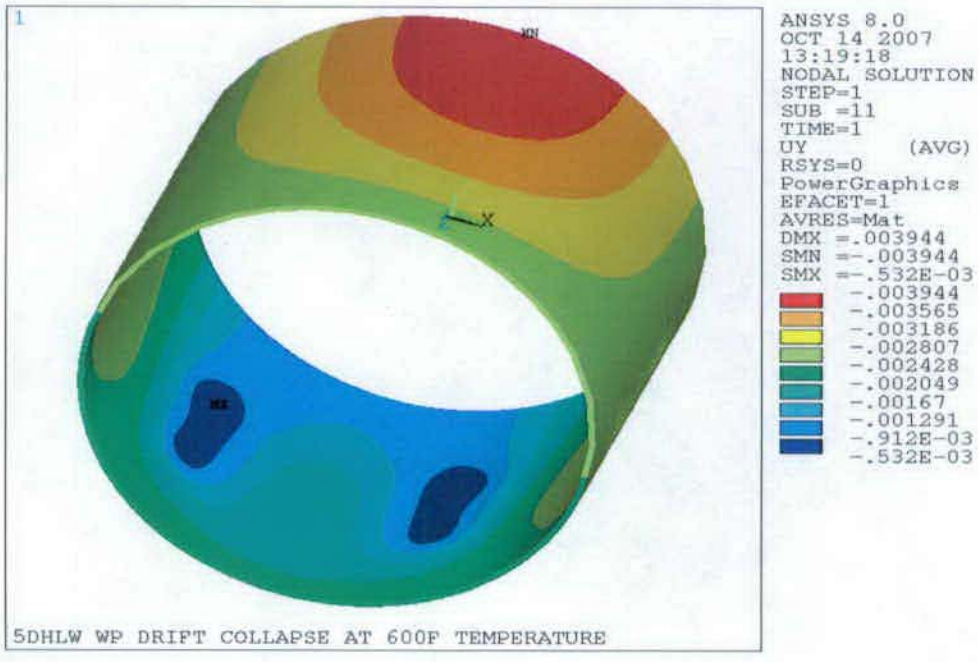

Figure 7-14. 5-DHLW OCB Peak Displacement [*m*] Contour Plot (Run 3B)

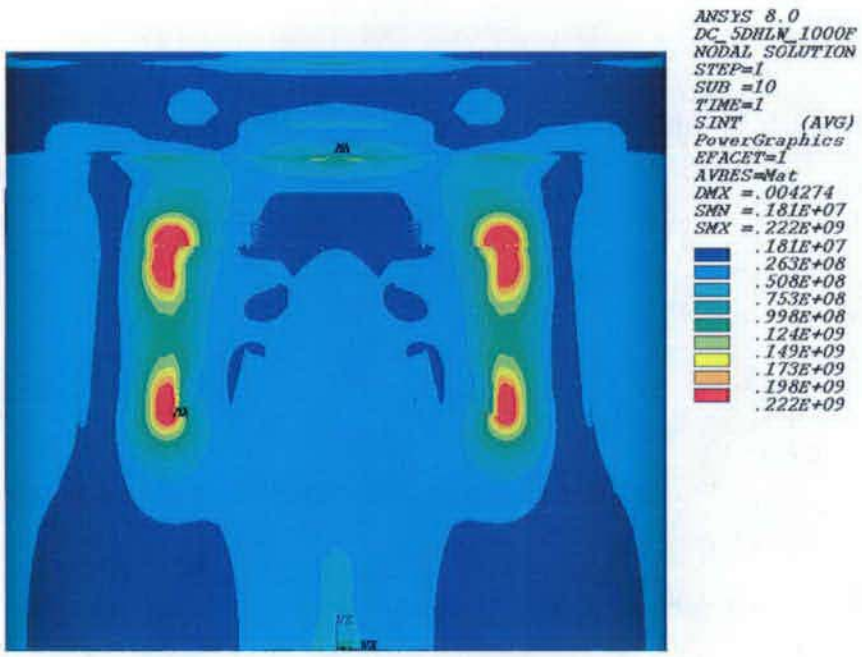

Figure 7-15. 5-DHLW OCB Peak Stress Intensity [*GPa*] Contour Plot (Run 4B)

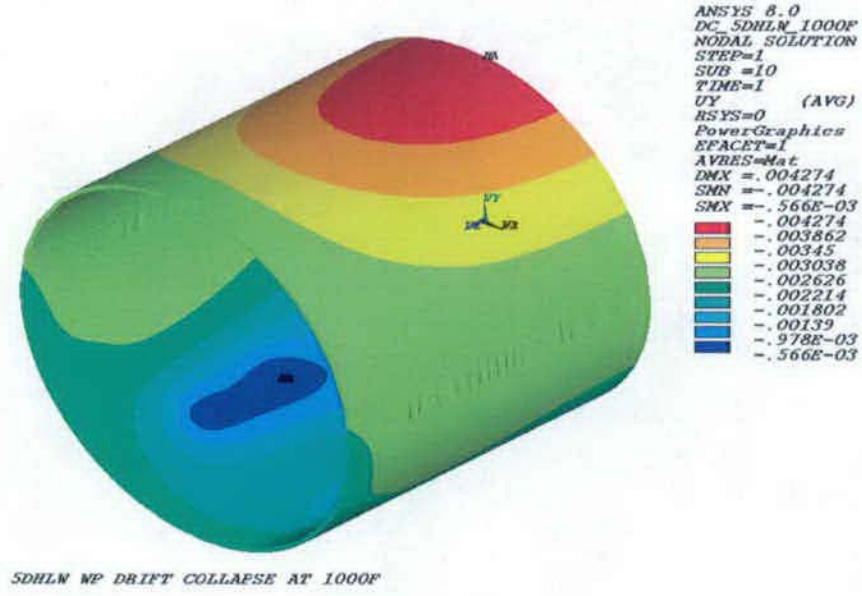

Figure 7-16. 5-DHLW OCB Peak Displacement [*m*] Contour Plot (Run 4B)

I. ATTACHMENT-I LIST OF FILES ON CD

```
Volume in drive D is 000-00C-MGR0-044
 Volume Serial Number is C2FC-505A

 Directory of D:\

10/29/2007  04:55 PM    <DIR>          000-00C-MGR0-04400-000-00A
               0 File(s)              0 bytes

 Directory of D:\000-00C-MGR0-04400-000-00A

10/29/2007  04:55 PM    <DIR>          .
10/30/2007  09:13 AM    <DIR>          ..
10/19/2007  03:46 PM    <DIR>          5DHLW
10/29/2007  04:43 PM            21,504 Mass_Verification.xls
10/19/2007  04:01 PM    <DIR>          TAD
10/29/2007  04:40 PM            17,920 Tangent_Modulus_Calculation.xls
               2 File(s)         39,424 bytes

 Directory of D:\000-00C-MGR0-04400-000-00A\5DHLW

10/19/2007  03:46 PM    <DIR>          .
10/29/2007  04:55 PM    <DIR>          ..
10/19/2007  03:37 PM            96,920 DC_5DHLW.tg
10/29/2007  04:25 PM    <DIR>          ROOM_TEMP
10/29/2007  04:24 PM    <DIR>          TEMP_1000F
10/29/2007  04:25 PM    <DIR>          TEMP_300F
10/29/2007  04:26 PM    <DIR>          TEMP_600F
               1 File(s)         96,920 bytes

 Directory of D:\000-00C-MGR0-04400-000-00A\5DHLW\ROOM_TEMP

10/29/2007  04:25 PM    <DIR>          .
10/19/2007  03:46 PM    <DIR>          ..
10/29/2007  04:23 PM        54,276,491 DC_5DHLW_RT.db.Z
10/19/2007  03:38 PM             1,359 DC_5DHLW_RT.mntr
10/19/2007  03:40 PM        12,612,261 Nodes_DY.txt
10/19/2007  03:40 PM         4,385,913 Nodes_SI.txt
               4 File(s)     71,276,024 bytes

 Directory of D:\000-00C-MGR0-04400-000-00A\5DHLW\TEMP_1000F

10/29/2007  04:24 PM    <DIR>          .
10/19/2007  03:46 PM    <DIR>          ..
10/29/2007  04:24 PM        54,278,627 DC_5DHLW_1000F.db.Z
10/19/2007  03:41 PM             1,541 DC_5DHLW_1000F.mntr
10/19/2007  03:43 PM        12,612,261 Nodes_DY.txt
10/19/2007  03:43 PM         4,385,913 Nodes_SI.txt
               4 File(s)     71,278,342 bytes

 Directory of D:\000-00C-MGR0-04400-000-00A\5DHLW\TEMP_300F

10/29/2007  04:25 PM    <DIR>          .
10/19/2007  03:46 PM    <DIR>          ..
```

```
10/29/2007  04:25 PM        54,275,807 DC_5DHLW_300F.db.Z
10/19/2007  03:44 PM             2,354 DC_5DHLW_300F.mntr
10/19/2007  03:46 PM        12,612,261 Nodes_DY.txt
10/19/2007  03:46 PM        19,897,628 Nodes_SI.txt
               4 File(s)     86,788,050 bytes

 Directory of D:\000-00C-MGR0-04400-000-00A\5DHLW\TEMP_600F

10/29/2007  04:26 PM    <DIR>          .
10/19/2007  03:46 PM    <DIR>          ..
10/29/2007  04:26 PM        54,278,161 DC_5DHLW_600F.db.Z
10/19/2007  03:47 PM             2,263 DC_5DHLW_600F.mntr
10/19/2007  03:48 PM        12,612,261 Nodes_DY.txt
10/19/2007  03:48 PM         4,385,913 Nodes_SI.txt
               4 File(s)     71,278,598 bytes

 Directory of D:\000-00C-MGR0-04400-000-00A\TAD

10/19/2007  04:01 PM    <DIR>          .
10/29/2007  04:55 PM    <DIR>          ..
10/19/2007  03:48 PM            79,209 DC_RT.tg
10/29/2007  04:31 PM    <DIR>          ROOM_TEMP
10/29/2007  04:36 PM    <DIR>          TEMP_1000F
10/29/2007  04:31 PM    <DIR>          TEMP_300F
10/29/2007  04:32 PM    <DIR>          TEMP_600F
               1 File(s)         79,209 bytes

 Directory of D:\000-00C-MGR0-04400-000-00A\TAD\ROOM_TEMP

10/29/2007  04:31 PM    <DIR>          .
10/19/2007  04:01 PM    <DIR>          ..
10/29/2007  04:31 PM        53,639,642 DC_RT.db.Z
10/19/2007  03:49 PM             1,541 DC_RT.mntr
10/19/2007  03:51 PM        12,612,261 Nodes_DY.txt
10/19/2007  03:51 PM         4,373,035 Nodes_SI.txt
               4 File(s)     70,626,479 bytes

 Directory of D:\000-00C-MGR0-04400-000-00A\TAD\TEMP_1000F

10/29/2007  04:36 PM    <DIR>          .
10/19/2007  04:01 PM    <DIR>          ..
10/29/2007  04:36 PM        53,644,076 DC_1000F.db.Z
10/19/2007  03:52 PM             1,359 DC_1000F.mntr
10/19/2007  03:54 PM        12,612,261 Nodes_DY.txt
10/19/2007  03:54 PM         4,373,035 Nodes_SI.txt
               4 File(s)     70,630,731 bytes

 Directory of D:\000-00C-MGR0-04400-000-00A\TAD\TEMP_300F

10/29/2007  04:31 PM    <DIR>          .
10/19/2007  04:01 PM    <DIR>          ..
10/29/2007  04:31 PM        53,644,589 DC_300F.db.Z
10/19/2007  03:59 PM             1,541 DC_300F.mntr
10/19/2007  04:01 PM        12,612,261 Nodes_DY.txt
10/19/2007  04:01 PM         4,373,035 Nodes_SI.txt
               4 File(s)     70,631,426 bytes
```

Directory of D:\000-00C-MGR0-04400-000-00A\TAD\TEMP_600F

```
10/29/2007  04:32 PM    <DIR>          .
10/19/2007  04:01 PM    <DIR>          ..
10/29/2007  04:32 PM        53,637,492 DC_600F.db.Z
10/19/2007  04:01 PM             1,359 DC_600F.mntr
10/19/2007  04:03 PM        12,612,261 Nodes_DY.txt
10/19/2007  04:03 PM         4,373,035 Nodes_SI.txt
               4 File(s)     70,624,147 bytes

    Total Files Listed:
              36 File(s)    583,349,350 bytes
              33 Dir(s)               0 bytes free
```

OFFICE OF CIVILIAN RADIOACTIVE WASTE MANAGEMENT
SPECIAL INSTRUCTION SHEET

1. QA: QA
Page 1 of 1

This is a placeholder page for records that cannot be scanned.

2. Record Date	3. Accession Number
10/30/2007	Att. To: ENG.20071030.0041
4. Author Name(s)	5. Authorization Organization
Sripathi Nilkar; Nakachew Alemu	BSC/Subsurface/Thermal/Structural

6. Title/Description
Drift Collapse Weight and Thermal Loading of TAD and 5-DHLW/DOE SNF Short Co-Disposal Waste Packages

7. Document Number(s)	8. Version Designator
000-00C-MGR0-04400-000	00A
9. Document Type	10. Medium
Media	2 CD's

11. Access Control Code
PUB

12. Traceability Designator
000-00C-MGR0-04400-000-00A

13. Comments
CD's: 1 Original
1 Copy

Validation of complete file transferred. All files copied. Software used: ANSYS V8.0; Microsoft Office Excel 2003.

14. RPC Electronic Media Verification

XREF MOL.20071106.0075

NOV 07 2007 T Church /BSC-BS

MD5 Validation

THIS IS AN ELECTRONIC ATTACHMENT

```
 Volume in drive D is 000-00C-MGR0-044
 Volume Serial Number is C2FC-505A

 Directory of D:\

10/29/2007  04:55 PM    <DIR>          000-00C-MGR0-04400-000-00A
               0 File(s)              0 bytes

 Directory of D:\000-00C-MGR0-04400-000-00A

10/29/2007  04:55 PM    <DIR>          .
10/30/2007  09:13 AM    <DIR>          ..
10/19/2007  03:46 PM    <DIR>          5DHLW
10/29/2007  04:43 PM            21,504 Mass_Verification.xls
10/19/2007  04:01 PM    <DIR>          TAD
10/29/2007  04:40 PM            17,920 Tangent_Modulus_Calculation.xls
               2 File(s)         39,424 bytes

 Directory of D:\000-00C-MGR0-04400-000-00A\5DHLW

10/19/2007  03:46 PM    <DIR>          .
10/29/2007  04:55 PM    <DIR>          ..
10/19/2007  03:37 PM            96,920 DC_5DHLW.tg
10/29/2007  04:25 PM    <DIR>          ROOM_TEMP
10/29/2007  04:24 PM    <DIR>          TEMP_1000F
10/29/2007  04:25 PM    <DIR>          TEMP_300F
10/29/2007  04:26 PM    <DIR>          TEMP_600F
               1 File(s)         96,920 bytes

 Directory of D:\000-00C-MGR0-04400-000-00A\5DHLW\ROOM_TEMP

10/29/2007  04:25 PM    <DIR>          .
10/19/2007  03:46 PM    <DIR>          ..
10/29/2007  04:23 PM        54,276,491 DC_5DHLW_RT.db.Z
10/19/2007  03:38 PM             1,359 DC_5DHLW_RT.mntr
10/19/2007  03:40 PM        12,612,261 Nodes_DY.txt
10/19/2007  03:40 PM         4,385,913 Nodes_SI.txt
               4 File(s)     71,276,024 bytes

 Directory of D:\000-00C-MGR0-04400-000-00A\5DHLW\TEMP_1000F

10/29/2007  04:24 PM    <DIR>          .
10/19/2007  03:46 PM    <DIR>          ..
10/29/2007  04:24 PM        54,278,627 DC_5DHLW_1000F.db.Z
10/19/2007  03:41 PM             1,541 DC_5DHLW_1000F.mntr
10/19/2007  03:43 PM        12,612,261 Nodes_DY.txt
10/19/2007  03:43 PM         4,385,913 Nodes_SI.txt
               4 File(s)     71,278,342 bytes

 Directory of D:\000-00C-MGR0-04400-000-00A\5DHLW\TEMP_300F

10/29/2007  04:25 PM    <DIR>          .
10/19/2007  03:46 PM    <DIR>          ..
10/29/2007  04:25 PM        54,275,807 DC_5DHLW_300F.db.Z
10/19/2007  03:44 PM             2,354 DC_5DHLW_300F.mntr
10/19/2007  03:46 PM        12,612,261 Nodes_DY.txt
10/19/2007  03:46 PM        19,897,628 Nodes_SI.txt
               4 File(s)     86,788,050 bytes

 Directory of D:\000-00C-MGR0-04400-000-00A\5DHLW\TEMP_600F

10/29/2007  04:26 PM    <DIR>          .
10/19/2007  03:46 PM    <DIR>          ..
```

```
                                    dir.txt
10/29/2007  04:26 PM        54,278,161 DC_5DHLW_600F.db.Z
10/19/2007  03:47 PM             2,263 DC_5DHLW_600F.mntr
10/19/2007  03:48 PM        12,612,261 Nodes_DY.txt
10/19/2007  03:48 PM         4,385,913 Nodes_SI.txt
               4 File(s)     71,278,598 bytes

 Directory of D:\000-00C-MGR0-04400-000-00A\TAD

10/19/2007  04:01 PM    <DIR>          .
10/29/2007  04:55 PM    <DIR>          ..
10/19/2007  03:48 PM            79,209 DC_RT.tg
10/29/2007  04:31 PM    <DIR>          ROOM_TEMP
10/29/2007  04:36 PM    <DIR>          TEMP_1000F
10/29/2007  04:31 PM    <DIR>          TEMP_300F
10/29/2007  04:32 PM    <DIR>          TEMP_600F
               1 File(s)         79,209 bytes

 Directory of D:\000-00C-MGR0-04400-000-00A\TAD\ROOM_TEMP

10/29/2007  04:31 PM    <DIR>          .
10/19/2007  04:01 PM    <DIR>          ..
10/29/2007  04:31 PM        53,639,642 DC_RT.db.Z
10/19/2007  03:49 PM             1,541 DC_RT.mntr
10/19/2007  03:51 PM        12,612,261 Nodes_DY.txt
10/19/2007  03:51 PM         4,373,035 Nodes_SI.txt
               4 File(s)     70,626,479 bytes

 Directory of D:\000-00C-MGR0-04400-000-00A\TAD\TEMP_1000F

10/29/2007  04:36 PM    <DIR>          .
10/19/2007  04:01 PM    <DIR>          ..
10/29/2007  04:36 PM        53,644,076 DC_1000F.db.Z
10/19/2007  03:52 PM             1,359 DC_1000F.mntr
10/19/2007  03:54 PM        12,612,261 Nodes_DY.txt
10/19/2007  03:54 PM         4,373,035 Nodes_SI.txt
               4 File(s)     70,630,731 bytes

 Directory of D:\000-00C-MGR0-04400-000-00A\TAD\TEMP_300F

10/29/2007  04:31 PM    <DIR>          .
10/19/2007  04:01 PM    <DIR>          ..
10/29/2007  04:31 PM        53,644,589 DC_300F.db.Z
10/19/2007  03:59 PM             1,541 DC_300F.mntr
10/19/2007  04:01 PM        12,612,261 Nodes_DY.txt
10/19/2007  04:01 PM         4,373,035 Nodes_SI.txt
               4 File(s)     70,631,426 bytes

 Directory of D:\000-00C-MGR0-04400-000-00A\TAD\TEMP_600F

10/29/2007  04:32 PM    <DIR>          .
10/19/2007  04:01 PM    <DIR>          ..
10/29/2007  04:32 PM        53,637,492 DC_600F.db.Z
10/19/2007  04:01 PM             1,359 DC_600F.mntr
10/19/2007  04:03 PM        12,612,261 Nodes_DY.txt
10/19/2007  04:03 PM         4,373,035 Nodes_SI.txt
               4 File(s)     70,624,147 bytes

     Total Files Listed:
              36 File(s)    583,349,350 bytes
              33 Dir(s)               0 bytes free
```